MIKE 3 Flow Model

Hydrodynamic Module

Scientific Documentation

DHI headquarters
Agern Allé 5
DK-2970 Hørsholm
Denmark

+45 4516 9200 Telephone
+45 4516 9333 Support
+45 4516 9292 Telefax

mike@dhigroup.com
www.mikepoweredbydhi.com

PLEASE NOTE

CONTENTS

MIKE 3 Flow Model
Hydrodynamic Module
Scientific Documentation

1 Introduction

The present Scientific Documentation aims at giving an in-depth description of the equations and numerical formulation used in the Hydrodynamic Module of MIKE 3.

The non-hydrostatic version is described in the present documentation. For details on the hydrostatic version of MIKE 3, see MIKE 3 Flow Model - Hydrostatic Version - Scientific Documentation.

First the main equations and the numerical algorithms applied in the model are described. This is followed by a number of sections giving the physical, mathematical and numerical background for each of the terms in the main equations.

2 Main Equations

The hydrodynamic model in MIKE 3 is a general numerical modelling system for simulation of flows in estuaries, bays and coastal areas as well as in oceans. It simulates unsteady three-dimensional flows taking into account density variations, bathymetry and external forcing such as meteorology, tidal elevations, currents and other hydrographic conditions.

In a three-dimensional hydrodynamic model for flow of Newtonian fluids, the following elements are required

- mass conservation
- momentum conservation
- conservation of salinity and temperature
- equation of state relating local density to salinity, temperature and pressure

Thus, the governing equations consist of seven equations with seven unknowns.

The mathematical foundation in MIKE 3 is the mass conservation equation, the Reynolds-averaged Navier-Stokes equations in three dimensions, including the effects of turbulence and variable density, together with the conservation equations for salinity and temperature.

$$\frac{1}{\rho c_s^2}\frac{\partial P}{\partial t} + \frac{\partial u_j}{\partial x_j} = SS \tag{2.1}$$

$$\frac{\partial u_i}{\partial t} + \frac{\partial (u_i u_j)}{\partial x_j} + 2\Omega_{ij} u_j = -\frac{1}{\rho}\frac{\partial P}{\partial x_i} + g_i + \frac{\partial}{\partial x_j}\left(\nu_T \left\{ \frac{\partial u_i}{\partial x_j} + \frac{\partial u_j}{\partial x_i} \right\} - \frac{2}{3}\delta_{ij} k \right) + u_i SS \tag{2.2}$$

$$\frac{\partial S}{\partial t} + \frac{\partial}{\partial x_j}(S u_j) = \frac{\partial}{\partial x_j}\left(D_s \frac{\partial S}{\partial x_j} \right) + SS \tag{2.3}$$

$$\frac{\partial T}{\partial t} + \frac{\partial}{\partial x_j}(T u_j) = \frac{\partial}{\partial x_j}\left(D_T \frac{\partial T}{\partial x_j} \right) + SS \tag{2.4}$$

where ρ is the local density of the fluid, c_s the speed of sound in seawater, u_i the velocity in the x_i-direction, Ω_{ij} the Coriolis tensor, P the fluid pressure, g_i the gravitational vector, ν_T the turbulent eddy viscosity, δ Kronecker's delta, k the turbulent kinetic energy, S and T the salinity and temperature, D_S and D_T the associated dispersion coefficients and t

denotes the time. *SS* refers to the respective source-sink terms and thus differs from equation to equation.

The salinity, temperature and pressure are related to the density through the UNESCO definitions (UNESCO 1981).

In most three-dimensional models the fluid is assumed incompressible. However using the divergence-free (incompressible) mass equation, the set of equations will inevitably form a mathematical ill-conditioned problem. In most models this is solved through the hydrostatic pressure assumption whereby the pressure is replaced by information about the surface elevation. In order to retain the full vertical momentum equation an alternative approach has been adopted in MIKE 3. This approach is known as the artificial compressibility method (Chorin 1967, Rasmussen 1993) in which an artificial compressibility term is introduced whereby the set of equations mathematically speaking becomes hyperbolic dominated. The compressibility is discussed further in Section 10.

Equations (2.1) and (2.2) are referred to as the hydrodynamic equations whereas Equations (2.3) and (2.4) are referred to as advection-dispersion equations in the following sections. The two first equations are solved in the hydrodynamic module and similarly the advection-dispersion equations are solved using the advection-dispersion module.

3 Introduction to Numerical Formulation

The hydrodynamics module of MIKE 3 makes use of the so-called Alternating Direction Implicit (ADI) technique to integrate the equations for mass and momentum conservation in the space-time domain. The equation matrices, which result for each direction and each individual grid line, are resolved by a Double Sweep (DS) algorithm.

The hydrodynamic module has the following properties:

- zero numerical mass and momentum falsification and negligible numerical energy falsification, over the range of practical applications, through centring of all difference terms and dominant coefficients, achieved without resort to iteration
- discretised on the Arakawa C-grid aiming at a second-order accuracy on all terms, i.e. "second-order" in terms of the discretisation error in a Taylor series expansion
- a well-conditioned solution algorithm providing accurate, reliable and fast operation

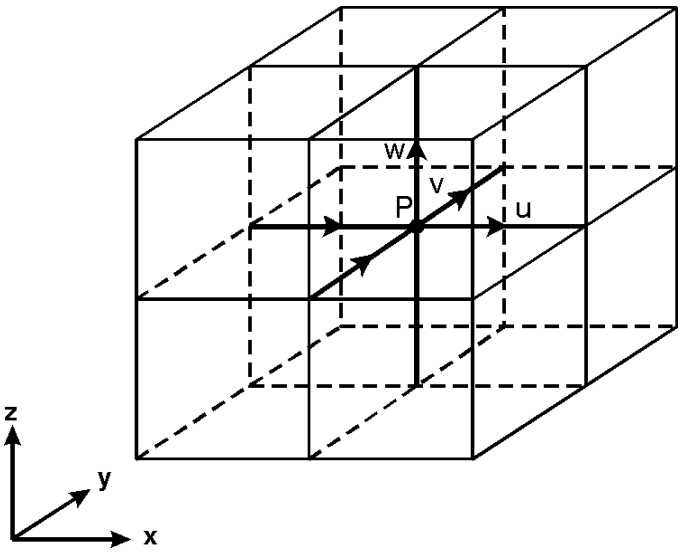

Figure 3.1 Difference grid in x, y and z-space

The difference terms are expressed on a staggered grid in x, y and z-space as shown in Figure 3.1. This grid is known as the Arakawa C-grid.

Time centring of the four hydrodynamic equations is achieved as sketched in Figure 3.2.

The equations are solved in one-dimensional sweeps, alternating between x, y and z directions. In the x-sweep the continuity

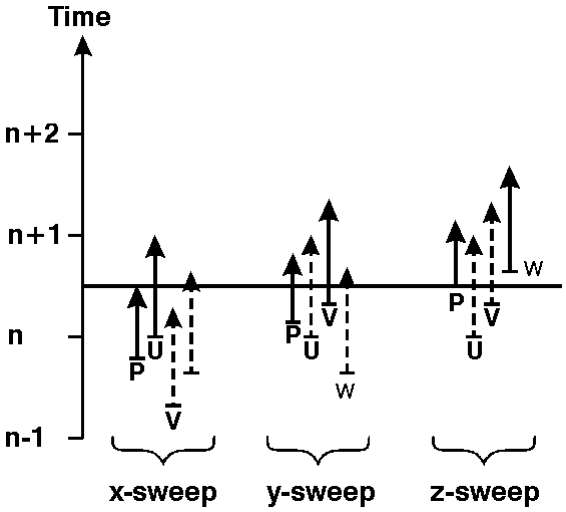

Figure 3.2 Time centring

and x-momentum equations are solved, taking *P* from *n-1/6* to *n+½* and *u* from *n* to *n+1*. For the terms involving *v* and *w*, the two levels of old, known values are used, i.e. *n-2/3* and *n+1/3* for the v-velocity and *n-1/3* and *n+2/3* for the w-velocity.

In the y-sweep, the continuity and y-momentum equations are solved taking *P* from *n+1/6* to *n+5/6* and *v* from *n+1/3* to *n+4/3*, while terms involving *u* use the values of *u* just calculated in the x-sweep at *n* and *n+1* and for terms in *w* the two time levels *n-1/3* and *n+2/3*.

Eventually in the z-sweep, the continuity and z-momentum equations are solved taking *P* from *n+3/6* to *n+7/6* and *w* from *n+2/3* to *n+5/3*, while terms involving *u* and *v* use the values at their latest calculated time levels, i.e. *n* and *n+1* for the u-velocity and *n+1/3* and *n+4/3* for the v-velocity.

Adding the three sweeps together gives "perfect" time centring at *n+½*, i.e. the time centring is given by a balanced sequence of operations. The word perfect has been put in quotation marks because it is not possible to achieve perfect time centring of the cross derivatives in the momentum equation. The best approximation, without resorting to iteration (which has its own problems), is to use a "side feeding" technique.

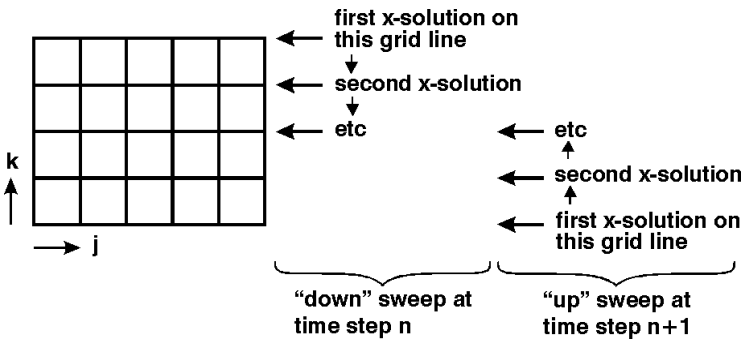

Figure 3.3 Side-feeding

At one time step the x-sweep solutions are performed in the order of decreasing y- and z-directions, hereafter called a "down" sweep, and in the next time step in the order of increasing y- and z-direction, the "up" sweep.

During a "down" sweep, the cross derivative ∂u/∂y and ∂u/∂z can be expressed in terms of $u^{n+1}_{j,k+1,l}$ on the "up" side and $u^{n}_{j,k-1,l}$ on the "down" side for the ∂u/∂y term and similarly the ∂u/∂z term can be expressed in terms of $u^{n+1}_{j,k,l+1}$ on the "up" side and $u^{n}_{j,k,l-1}$ on the "down" side. During an "up" sweep, the indices are swapped. In this way an approximate time centring of ∂u/∂y and ∂u/∂z at n+½ can be achieved, albeit with the possibility of developing some oscillations (zigzagging).

The use of side feeding for the individual cross differentials is described in more detail in the following sections.

This structure implies that the pressure just calculated in a sweep can be used as the old pressure in two sweeps ahead, i.e. the pressure from the x-sweep can be used in the z-sweep, which in turn can be used in the y-sweep,etc. To exchange information between the individual sweeps slightly faster MIKE 3 uses a time filtering of the pressure such that the pressure calculated in a sweep is used in the immediately following sweep.

Finally, it should also be mentioned that it is not always possible to achieve a perfect time centring of the coefficients on the differentials.

Centring in space is not generally a problem as will be seen in the next sections.

The mass and momentum equations thus expressed in a one-dimensional sweep for a sequence of grid points lead to a three-diagonal matrix

$$MV^{n+1} = W^{n} \tag{3.1}$$

$$A_j \cdot u^{n+1}_{j-1} + B_j \cdot P^{n+½}_{j} + C_j \cdot u^{n+1}_{j} = D_j\Big|_{k,l}$$

$$A^*_j \cdot P^{n+½}_{j} + B^*_j \cdot u^{n+1}_{j} + C^*_j \cdot P^{n+½}_{j+1} = D^*_j\Big|_{k,l} \tag{3.2}$$

where the coefficients *A, B, C, D* and A^*, B^*, C^*, D^* are all expressed in “known” quantities. Note that Equation (3.2) is here shown for the x-direction but equivalent structures exist for the y- and z-directions.

The system (3.1) is then solved by the well-known Double Sweep algorithm. For reference one may see, for example, Richtmeyer & Morton 1967. In developing the algorithm one postulates that these exist relations

$$u^{n+1}_{j} = E^*_j \cdot P^{n+½}_{j} + F^*_j$$

$$p^{n+½}_{j+1} = E_j \cdot u^{n+1}_{j} + F_{j+1} \tag{3.3}$$

Substituting these relations back into Equation (3.2) gives recurrence relations for *E, F,* E^* and F^*.

It is clear that once a pair of E_j, F_j values is known (or E^*_{j+1}, F^*_{j+1}) then all E, F and E^*, F^* coefficients can be computed for decreasing j. Introducing the right-hand boundary condition into one of the Equations (3.2) starts the recurrence computation for E, F and E^*, F^* - the E, F-sweep. Introducing the left-hand boundary condition in Equation (3.3) starts the complimentary sweep in which P and u are compared.

$$E^*_j = \frac{-A^*_j}{B^*_j + C^*_j \cdot E_j}$$

$$F^*_j = \frac{D^*_j - C^*_j \cdot F_j}{B^*_j + C^*_j \cdot E_j} \qquad (3.4)$$

$$E_{j-1} = \frac{-A_j}{B_j + C_j \cdot E^*_j}$$

$$F_{j-1} = \frac{D_j - C_j \cdot F^*_j}{B_j + C_j \cdot E^*_j}$$

As discussed earlier, sweeps may be carried out with a decreasing complimentary coordinates or increasing complimentary coordinates. This is organised in the cycle shown in Figure 3.4.

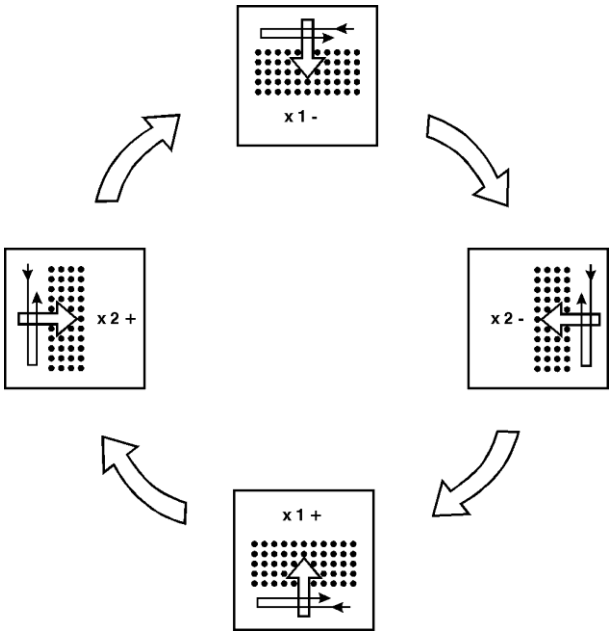

Figure 3.4 Cycle of computational sweeps

In Section 6 the numerical properties of the difference scheme in terms of amplification and propagation errors are discussed. Before this, we shall present various difference approximations.

4 Difference Approximations for Points away from Coast

We shall mainly look at the mass and momentum equations in the x-direction. As the mass equation in the y- and z-directions influences the centring of the x-mass equation, we shall also consider the difference approximation of these equations. The momentum equation in the y- and z-directions are analogous to the momentum equation in the x-direction and are, accordingly, omitted here. The boundary conditions for the momentum equation in the z-direction, however, are (in most applications) different from its counterparts in the two other directions. These are discussed further in Section 8.

4.1 Mass Equation in the x-Direction

The mass equation reads

$$\frac{1}{\rho c_s^2}\frac{\partial P}{\partial t}+\frac{\partial u}{\partial x}+\frac{\partial v}{\partial y}+\frac{\partial w}{\partial z}=SS \tag{4.1}$$

The x-, y- and z-sweeps are organised in a special cycle as shown in the preceding section. In Section 6 it is shown how the computation proceeds in time and how the equations are time centred.

In order to fully understand the balance between the difference approximations employed in the various sweeps it is necessary to read Section6 in conjunction with the following sections. For the moment it is sufficient to say that the x-mass and x-momentum equations bring *P* from time level *n-1/6* to *n+½* while bringing *u* from *n* to *n+1*. Together with the y- and z-mass equations the terms are centred at *n+½*.

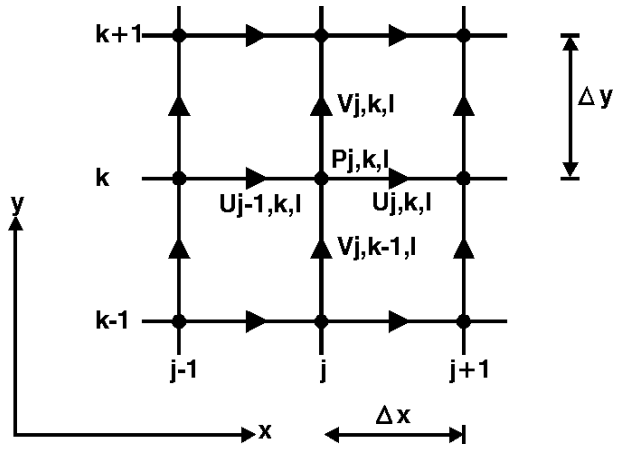

Figure 4.1 Grid notation mass equation, horizontal view

The grid notation for the horizontal plane is shown in Figure 4.1. A similar definition is used in the vertical. Thus, *u* and *v* may be replaced by any combination of *u, v* and *w* as appropriate. Hence, by definition Equation (4.1) becomes

$$\frac{1}{\rho_{j,k,l}c_s^2}\left(\frac{P^{n+\frac{1}{2}}-P^{n-\frac{1}{6}}}{\frac{2}{3}\Delta t}\right)_{j,k,l}+\frac{1}{2}\left\{\left(\frac{u_j-u_{j-1}}{\Delta x}\right)^{n+1}+\left(\frac{u_j-u_{j-1}}{\Delta x}\right)^{n}\right\}_{k,l}$$

$$+\frac{1}{2}\left\{\left(\frac{v_k-v_{k-1}}{\Delta y}\right)^{n+\frac{1}{3}}+\left(\frac{v_k-v_{k-1}}{\Delta y}\right)^{n-\frac{2}{3}}\right\}_{j,l} \qquad (4.2)$$

$$+\frac{1}{2}\left\{\left(\frac{w_l-w_{l-1}}{\Delta z}\right)^{n+\frac{2}{3}}+\left(\frac{w_l-w_{l-1}}{\Delta z}\right)^{n-\frac{1}{3}}\right\}_{j,k} = SS$$

4.2 Mass Equation in the y-Direction

The y sweep immediately following the x-sweep, for which the mass equation was just described, brings *P* from time level *n+1/6* to level *n+5/6* and helps to centre the x-mass and x-momentum equations. With the grid notation of Figure 4.1, Equation (4.1) becomes

$$\frac{1}{\rho_{j,k,l}c_s^2}\left(\frac{P^{n+\frac{5}{6}}-P^{n+\frac{1}{6}}}{\frac{2}{3}\Delta t}\right)_{j,k,l}+\frac{1}{2}\left\{\left(\frac{u_j-u_{j-1}}{\Delta x}\right)^{n+1}+\left(\frac{u_j-u_{j-1}}{\Delta x}\right)^{n}\right\}_{k,l}$$

$$+\frac{1}{2}\left\{\left(\frac{v_k-v_{k-1}}{\Delta y}\right)^{n+\frac{4}{3}}+\left(\frac{v_k-v_{k-1}}{\Delta y}\right)^{n+\frac{1}{3}}\right\}_{j,l} \qquad (4.3)$$

$$+\frac{1}{2}\left\{\left(\frac{w_l-w_{l-1}}{\Delta z}\right)^{n+\frac{2}{3}}+\left(\frac{w_l-w_{l-1}}{\Delta z}\right)^{n-\frac{1}{3}}\right\}_{j,k} = SS$$

4.3 Mass Equation in the z-Direction

Eventually the z sweep immediately following the y-sweep brings *P* from time level *n+3/6* to level *n+7/6*. Equation (4.1) thus becomes:

$$\frac{1}{\rho_{j,k,l}c_s^2}\left(\frac{P^{n+\frac{7}{6}}-P^{n+\frac{3}{6}}}{\frac{2}{3}\Delta t}\right)_{j,k,l}+\frac{1}{2}\left\{\left(\frac{u_j-u_{j-1}}{\Delta x}\right)^{n+1}+\left(\frac{u_j-u_{j-1}}{\Delta x}\right)^{n}\right\}_{k,l}$$

$$+\frac{1}{2}\left\{\left(\frac{v_k-v_{k-1}}{\Delta y}\right)^{n+\frac{4}{3}}+\left(\frac{v_k-v_{k-1}}{\Delta y}\right)^{n+\frac{1}{3}}\right\}_{j,l} \tag{4.4}$$

$$+\frac{1}{2}\left\{\left(\frac{w_l-w_{l-1}}{\Delta z}\right)^{n+\frac{5}{3}}+\left(\frac{w_l-w_{l-1}}{\Delta z}\right)^{n+\frac{2}{3}}\right\}_{j,k} = SS$$

We will not discuss truncation errors at this point. As the approximations are based on a multilevel difference method, centring of terms and the evaluation of truncation errors should be considered in conjunction with a certain set of equations. We will revert to this point in Section 6.

4.4 Momentum Equation in the x-Direction

4.4.1 General

The x-component of the momentum equation reads

$$\frac{\partial u}{\partial t}+\frac{\partial}{\partial x}\left(u^2\right)+\frac{\partial}{\partial y}(uv)+\frac{\partial}{\partial z}(uw)$$

$$+2\omega\left(v\sin(\varphi)-w\cos(\varphi)\sin(\lambda)\right)+\frac{1}{\rho}\frac{\partial P}{\partial x} \tag{4.5}$$

$$+\frac{\partial}{\partial x}\left(2\nu_T\frac{\partial u}{\partial x}\right)-\frac{\partial}{\partial y}\left(\nu_T\left\{\frac{\partial u}{\partial y}+\frac{\partial v}{\partial x}\right\}\right)-\frac{\partial}{\partial z}\left(\nu_T\left\{\frac{\partial u}{\partial z}+\frac{\partial w}{\partial x}\right\}\right)$$

$$+\frac{2}{3}\frac{\partial k}{\partial x}-uSS = 0$$

in which ω is the angular velocity of the Earth, φ the latitude and λ the longitude. We shall develop the difference forms by considering the various terms one by one.

The following basic principle is used for the finite difference approximations of the x-momentum:

Terms in Equation (4.5) should be time centred at *n+½* and space centred at the location corresponding to $u_{j,k,l}$ in the space-staggered grid. The grid notation is shown in Figure 4.2.

4.4.2 The Time Derivation Term

The straightforward finite difference approximation to the time derivative term is

$$\frac{\partial u}{\partial t} \approx \left(\frac{u^{n+1} - u^n}{\Delta t} \right)_{j,k,l} \tag{4.6}$$

Using a Taylor series expansion centred at n+½ leads to

$$\frac{\partial u}{\partial t} = \left(\frac{u^{n+1} - u^n}{\Delta t} \right)_{j,k,l} - \frac{\Delta t^2}{24} \cdot \frac{\partial^3 u}{\partial t^3} + HOT \quad (Higher \quad Order \quad Terms) \tag{4.7}$$

The central differencing (in either time or space) has inherent second order accuracy. In the hydrodynamic simulations only the first term in Equation (4.7) is included in the scheme.

4.4.3 The Convective Terms

The convective terms of the x-component of the momentum equation read

$$\frac{\partial}{\partial x}(uu) + \frac{\partial}{\partial y}(uv) + \frac{\partial}{\partial z}(uw) \tag{4.8}$$

One way of approximating these terms would be to form spatially centred differences of time centred forms of the bracketed terms. For example the first term would read

$$\left[\left(\frac{\left(u^{n+1} + u^n\right)\left(u^{n+1} + u^n\right)}{4} \right)_{j+1,k,l} \left(\frac{\left(u^{n+1} + u^n\right)\left(u^{n+1} + u^n\right)}{4} \right)_{j-1,k,l} \right] \frac{1}{2\Delta x} \tag{4.9}$$

However, such an approximation necessitates iteration due to its non-linearity. Alternatively this term could be approximated as

$$\frac{\left(u^{n+1}\cdot u^{n}\right)_{j+1,k,l}\ \left(u^{n+1}\cdot u^{n}\right)_{j-1,k,l}}{2\Delta x} \tag{4.10}$$

In this way the term has been linearised in the resulting algebraic formulation. Truncation errors embedded in Equation (4.10) can be determined by the use of Taylor series expansions centred at *j,k,l* and *n+½*. This leads to

$$\frac{\partial u^2}{\partial x} = FDS - u\left[\frac{\Delta x^2}{3}\ \frac{\partial^3 u}{\partial x^3} + \Delta t^2\ \frac{\partial^3 u}{\partial x \partial t^2}\right] \tag{4.11}$$

$$+\ HOT\ (Higher\ \ Order\ \ Terms)$$

where FDS is given by Equation (4.10). Hence the approximation is of second-order accuracy.

As MIKE 3 uses a non-iterative procedure to advance the solution in time the non-linear terms all have to be linearised according to the principle of Equation (4.10) .

One will note that the difference form in Equation (4.10) in fact involves 5 diagonals in the matrix of difference equations, whereas we employ a "tri-diagonal" algorithm for its solution. One can extend the "tri-diagonal" algorithm to a "penta-diagonal" algorithm. Here we have chosen to reduce the form (4.10) to a tri-diagonal form by local substitution.

The difference approximation of the two remaining terms in Equation (4.8) will differ between an "up" sweep and a "down" sweep. We shall use "side feeding" as a mean to centre the terms at level *(n+½)* Δt.

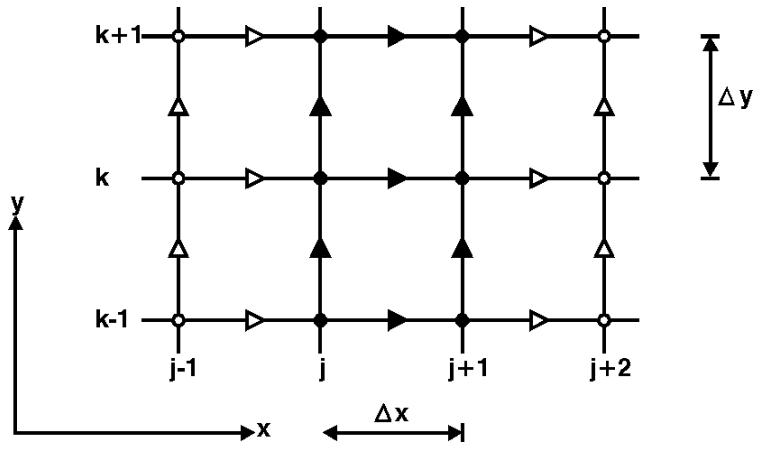

Figure 4.2 Grid notation: x-momentum equation

We write, referring to the grid notation of Figure 4.2,

$$\frac{\partial}{\partial y}(uv) \approx \left[\left(\frac{u_{k+1}^{a} + u_{k}^{b}}{2} \right)_{j,l} \cdot v_{j+\frac{1}{2},k,l}^{n+\frac{1}{2}} - \left(\frac{u_{k}^{a} + u_{k-1}^{b}}{2} \right)_{j,l} \cdot v_{j+\frac{1}{2},k-1,l}^{n+\frac{1}{2}} \right] \cdot \frac{1}{\Delta y} \tag{4.12}$$

where: $a = n+1$, $b = n$ for a "down" sweep
$a = n$, $b = n+1$ for an "up" sweep

$$v_{j+\frac{1}{2},k,l}^{n+\frac{1}{2}} = \frac{1}{2}\left(v_j + v_{j+1}\right)_{k,l}^{n+1/3}$$

$$v_{j+\frac{1}{2},k-1,l}^{n+\frac{1}{2}} = \frac{1}{2}\left(v_j + v_{j+1}\right)_{k-1,l}^{n+1/3} \tag{4.13}$$

The diagrams in Figure 4.3 and Figure 4.4 may illustrate how the cross terms are built.

Note that the main computation we are dealing with in this approximation of the x-momentum equation is in the x-direction. By "down" sweep or "up" sweep we mean in fact computational sweeps in the x-direction, carried out by decreasing or increasing *y* and *z*, respectively.

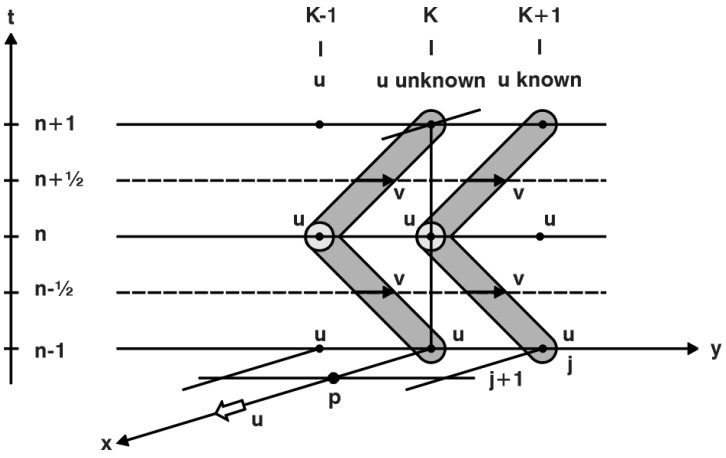

Figure 4.3 "Side-feeding" for the convective term ∂(uv)/∂y. u(n+1,j,k+1,l) known, calculated by a "down" sweep. u(n,j,k-1,l) known, calculated by an "up" sweep

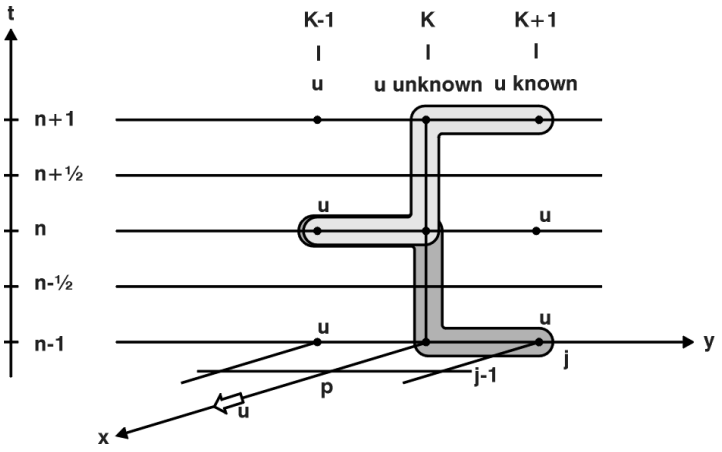

Figure 4.4 "Side-feeding" for the 2nd-order cross-derivative term. $\partial^2 u/\partial y^2$ for "down" sweep. $\partial^2 u/\partial y^2$ for an "up" sweep

Also note that the $v^{n+½}$ terms cannot be centred perfectly in time. It is one sixth of a time step back-centred. In fact, this will always be the case for one of the terms. In an x-sweep it is the v-component, in the y-sweep the w-component and in the z-sweep the u-component. The associated truncation error is again assessed by means of a Taylor series expansion, which leads to

$$\frac{\partial}{\partial y}(uv) = FDS + u\frac{\Delta t}{6}\frac{\partial^2 v}{\partial y \partial t} \pm \frac{1}{2}\Delta t\, v\frac{\partial^2 u}{\partial y \partial t} + HOT\ (Higher\ \ Order\ \ Terms) \tag{4.14}$$

where FDS is the right hand side of Equation (4.12). It is seen that the accuracy of this term is of the first order. The second term on the right hand side of Equation (4.14) is due to the back centring of v by $\Delta t/6$, whereas the third term is due to the side feeding. The sign of this term is positive for a "down" sweep and negative for an "up" sweep. Thus, "on average" the term cancels out. This is obviously not the case for the second term. Recall that during a y-sweep it will be the w-derivative term, which will be slightly back-centred and similarly the u-derivative term in a z-sweep.

The last term of Equation (4.8) yields

$$\frac{\partial}{\partial z}(uw) \approx \left[\left(\frac{u_{l+1}^a + u_l^b}{2}\right)_{j,k} \cdot w_{j+½,k,l}^{n+½} - \left(\frac{u_l^a + u_{l-1}^b}{2}\right)_{j,k} \cdot w_{j+½,k,l-1}^{n+½}\right] \cdot \frac{1}{\Delta z} \tag{4.15}$$

in which

$$w^{n+½}_{j+½,k,l} = \frac{5}{6}\frac{\left(w_j + w_{j+1}\right)^{n+\frac{2}{3}}_{k,l}}{2} + \frac{1}{6}\frac{\left(w_j + w_{j+1}\right)^{n-\frac{1}{3}}_{k,l}}{2}$$

$$w^{n+½}_{j+½,k,l-1} = \frac{5}{6}\frac{\left(w_j + w_{j+1}\right)^{n+\frac{2}{3}}_{k,l-1}}{2} + \frac{1}{6}\frac{\left(w_j + w_{j+1}\right)^{n-\frac{1}{3}}_{k,l-1}}{2} \quad (4.16)$$

a and *b* is referring to "up" sweep and "down" sweep directions like for the y-derivative term. A truncation error analysis of this approximation in terms of a Taylor series expansion yields

$$\frac{\partial}{\partial z}(uw) = FDS \pm \frac{1}{2}\Delta t \; w \; \frac{\partial^2 u}{\partial z \partial t} + HOT \; (Higher \;\; Order \;\; Terms) \quad (4.17)$$

with FDS given by Equation (4.15). Again the accuracy is of first order when considered at a certain time level but of second order "on average".

4.4.4 Coriolis Term

The Coriolis term

$$\Omega_{ij}u_i = 2\omega \begin{bmatrix} 0 & \sin(\phi) & \cos(\phi)\cos(\lambda) \\ -\sin(\phi) & 0 & \cos(\phi)\sin(\lambda) \\ \cos(\phi)\cos(\lambda) & -\cos(\phi)\sin(\lambda) & 0 \end{bmatrix} \begin{bmatrix} u \\ v \\ w \end{bmatrix} \quad (4.18)$$

is different for each of the directions. The principles of the finite difference approximations are the same, and accordingly only the discretisation in the x-momentum needs to be considered here. The two velocity components are approximated by

$$v^* = \frac{1}{4}\left(v_{j,k} + v_{j,k-1} + v_{j+1,k} + v_{j+1,k-1}\right)^{n+\frac{1}{3}}$$

$$w^* = \frac{5}{6}\frac{1}{4}\left(w_{j,l} + w_{j,l-1} + w_{j+1,l} + w_{j+1,l-1}\right)^{n+\frac{2}{3}} \quad (4.19)$$

$$+ \frac{1}{6}\frac{1}{4}\left(w_{j,l} + w_{j,l-1} + w_{j+1,l} + w_{j+1,l-1}\right)^{n-\frac{1}{3}}$$

The associated truncation errors are

$$v = FDS + \frac{\Delta t}{6}\frac{\partial v}{\partial t}$$

$$- \frac{1}{2}\left\{\left(\frac{\Delta x}{2}\right)^2 \frac{\partial^2 v}{\partial x^2} + \left(\frac{\Delta y}{2}\right)^2 \frac{\partial^2 v}{\partial y^2} + \left(\frac{\Delta x}{2}\right)^2 \frac{\partial^2 v}{\partial t^2}\right\}$$

$$+ HOT\ (Higher\ \ Order\ \ Terms) \qquad (4.20)$$

$$w = FDS - \frac{1}{2}\left\{\left(\frac{\Delta x}{2}\right)^2 \frac{\partial^2 w}{\partial x^2} + \left(\frac{\Delta z}{2}\right)^2 \frac{\partial^2 w}{\partial z^2} + 5\left(\frac{\Delta t}{6}\right)^2 \frac{\partial^2 w}{\partial t^2}\right\}$$

$$+ HOT\ (Higher\ \ Order\ \ Terms)$$

As for the convective term the v-velocity is back-centred $\Delta t/6$ of a time step which decreases the accuracy by one order. Recall that the velocity component which is back-centred differs from sweep to sweep.

4.4.5 The Pressure Term

The straightforward approximation to the pressure term reads

$$\frac{1}{\rho}\frac{\partial P}{\partial x} = \frac{1}{\frac{1}{2}\left(\rho_{j+1,k,l} + \rho_{j,k,l}\right)} \left(\frac{P_{j+1,k,l} - P_{j,k,l}}{\Delta x}\right)^{n+½} \qquad (4.21)$$

By virtue of the central difference in space this approximation has a second-order accuracy.

4.4.6 The Shear Terms

The discretisation of the shear terms in Equation (4.5) has many similarities with the convective terms. The approximation of the first term reads

$$\frac{\partial}{\partial x}\left(2\nu_T \frac{\partial u}{\partial x}\right) \approx \left[\frac{\left(u_{j+1}-u_j\right)_{k,l}^{n+1}+\left(u_{j+1}-u_j\right)_{k,l}^{n}}{\Delta x}\nu_{Tj+1,k,l} - \frac{\left(u_j-u_{j-1}\right)_{k,l}^{n+1}+\left(u_j-u_{j-1}\right)_{k,l}^{n}}{\Delta x}\nu_{Tj,k,l}\right]\frac{1}{\Delta x} \tag{4.22}$$

where *a* and *b* again refer to the "down" sweep and an "up" sweep, respectively. The associated truncation error yields

$$\begin{aligned}\frac{\partial}{\partial x}\left\{2\nu_T \frac{\partial u}{\partial x}\right\} &= FDS - \left(\frac{\Delta x}{2}\right)^2 \frac{\partial^2 \nu_T}{\partial x^2}\frac{\partial^2 u}{\partial x^2} \\ &- \frac{1}{3}\Delta x^2 \frac{\partial \nu_t}{\partial x}\frac{\partial^3 u}{\partial x^3} - \left(\frac{\Delta t}{2}\right)^2 \frac{\partial \nu_T}{\partial x}\frac{\partial^3 u}{\partial x \partial t^2} \\ &- \frac{2}{3}\Delta x^2 \frac{\partial u}{\partial x}\frac{\partial^3 \nu_T}{\partial x^3} \\ &+ HOT\ \ (Higher\ \ Order\ \ Terms)\end{aligned} \tag{4.23}$$

Thus the accuracy of this term is of second order. The finite difference approximation for the two remaining terms reads

$$\frac{\partial}{\partial y}\left(\nu_T\left\{\frac{\partial u}{\partial y}+\frac{\partial v}{\partial x}\right\}\right) \approx$$

$$\left[\frac{\left(u_{k+1}^a-u_k^b\right)_{j,l}}{\Delta y}\nu_{Tj,k+½,l}^* - \frac{\left(u_k^a-u_{k-1}^b\right)_{j,l}}{\Delta y}\nu_{Tj,k-½,l}^*\right]\frac{1}{\Delta x} \tag{4.24}$$

$$+\left[\frac{\left(v_{j+1}-v_j\right)_{k,l}^{n+\frac{1}{3}}}{\Delta x}\nu_{Tj,k+½,l}^* - \frac{\left(v_{j+1}-v_j\right)_{k-1,l}^{n+\frac{1}{3}}}{\Delta x}\nu_{Tj,k-½,l}^*\right]\frac{1}{\Delta y}$$

$$\frac{\partial}{\partial z}\left(\nu_T\left\{\frac{\partial u}{\partial z}+\frac{\partial w}{\partial x}\right\}\right) \approx$$

$$\left[\frac{\left(u_{l+1}^{a}-u_{l}^{b}\right)_{j,k}}{\Delta z}\nu^{*}_{Tj,k,l+½}-\frac{\left(u_{l}^{a}-u_{l-1}^{b}\right)_{j,l}}{\Delta z}\nu^{*}_{Tj,k,l-½}\right]\frac{1}{\Delta z}$$

$$+\left[\frac{\frac{5}{6}\left(w_{j+1}-w_j\right)_{k,l}^{n+\frac{2}{3}}+\frac{1}{6}\left(w_{j+1}-w_j\right)_{k,l}^{n-\frac{1}{3}}}{\Delta x}\nu^{**}_{Tj,k,l-½}\right. \tag{4.25}$$

$$\left.-\frac{\frac{5}{6}\left(w_{j+1}-w_j\right)_{k,l-1}^{n+\frac{2}{3}}+\frac{1}{6}\left(w_{j+1}-w_j\right)_{k,l-1}^{n+\frac{1}{3}}}{\Delta x}\nu^{**}_{Tj,k,l-½}\right]\Delta z$$

where ν_T^* and ν_T^{**} are defined in Equation (5.5), see Section **Error! Reference source not found.**.

The truncation errors of these terms are more comprehensive than the others shown here and have therefore been omitted. However, it can be shown that the side feeding decreases the accuracy of these approximations by one order but reversing the sweep directions will "on average" increase the accuracy again. As $v^{n+1/3}$ is slightly off-centred in time this will also lead to persistent truncation error terms of first-order accuracy.

5 Special Difference Approximations for Points near a Coast

The cross-derivatives in the hydrodynamic equations pose a problem when the computational sweep passes near land. Clearly, concepts such as side feeding become difficult to use. Inaccuracies, asymmetric behaviour between the "up" sweep and the "down" sweep may, especially at corners, cause a persistent reduction in accuracy and possibly create instabilities.

Land boundaries are defined at velocity points, with the velocity away from the land boundary set to zero. If for the purpose of this discussion, we consider an x-sweep, one can define the three principal situations given in Figure 5.1 to Figure 5.3 as Case 1, 2 and 3. They are here shown at the "positive" or "north" side of the sweep but have, of course, their counterparts on the negative side. The principal situations can be combined to create situations as shown, for example, in Figure 5.4. The difference formulation along a land boundary when it is at an angle to the grid (Figure 5.5) is especially demanding.

In the following we shall show possible approximations for the principal cases of Figure 5.1 to Figure 5.3. The approximations for the other combinations are based on the same principles.

The terms that involve cross-derivatives are - considering an x-sweep - the $\partial v/\partial y$ and $\partial w/\partial z$ terms in the mass equation, the convective terms $\partial(uv)/\partial y$ and $\partial(uw)/\partial z$, and the shear terms $\partial(\nu_T\{\partial u/\partial y+\partial v/\partial x\})/\partial y$ and $\partial(\nu_T\{\partial u/\partial z+\partial w/\partial x\})/\partial z$ in the momentum equation. The $\partial v/\partial y$ and $\partial w/\partial z$ terms of the mass equation offer no problems as these terms are implicitly described in the definition of the land boundary. The other terms will be considered one by one.

5.1 Convective Term

Consider the general form (4.12) for a "down" sweep

$$\frac{\partial}{\partial y}(uv) \approx \left[\left(\frac{u_{k+1}^{n+1} + u_k^n}{2} \right)_{j,l} \cdot v_{j+½,k+½,l}^{n+½} - \left(\frac{u_k^{n+1} + u_{k-1}^n}{2} \right)_{j,l} \cdot v_{j+½,k-½,l}^{n+½} \right] \frac{1}{\Delta y} \tag{5.1}$$

with

$$\begin{aligned} v_{j+½,k+½,l}^{n+½} &= \left(v_j + v_{j+1}\right)_{k,l}^{n+\frac{1}{3}} \\ v_{j+½,k-1,l}^{n+½} &= \left(v_j + v_{j+1}\right)_{k-1,l}^{n+\frac{1}{3}} \end{aligned} \tag{5.2}$$

CASE 1: Land to "North"

In general we shall assume a simple reflection condition for u. That is u_{k+1} is assumed to be equal to u_k. We assume a flow situation as shown in Figure 5.6.

In fact, there is no obvious reason for this assumption to be more correct than, for example, the assumption of a distribution as given in Figure 5.6b. However, the distribution of Figure 5.6b would generally give a greater gradient. We have preferred the distribution of Figure 5.6a as it gives a smaller value. To allow for a more general formulation, however, slip factors can be applied such that

$$u_{k+1} = (slip - factor) \cdot u_k \tag{5.3}$$

where the slip factors can vary between -1 and 1. A slip factor of -1 is equivalent to a no-slip condition along the boundary whereas 1 is equivalent to a full-slip condition. These assumptions should be kept in mind in applications where $\partial u/\partial y$ becomes important at the land boundary. In most horizontal spatial descriptions that we are dealing with - Δx, Δy several tenths or hundreds of metres - the full-slip condition is a good approximation.

For Case 1 the reflection assumption, however, does not matter. The general form of (5.1) reduces to a reasonable approximation because $v_{j+½,k+½,l} = 0$.

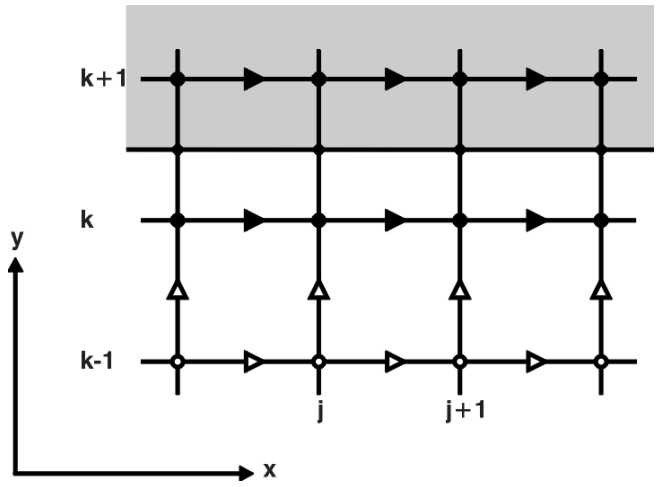

Figure 5.1 Special situations near Land. Land to “North” (CASE 1)

CASE 2: Corner - Exit

For *u* the reflection condition is used. The approximation of $v_{j+½,k+½,l}$ is more difficult. There are no evident assumptions to this case. Experience from regular grids has shown that, in general, the assumption that $v_{j+1,k+1,l} \approx 0$ gives good results. With this assumption $v_{j+½,k+½,l}$ can be approximated by the general expression (5.2).

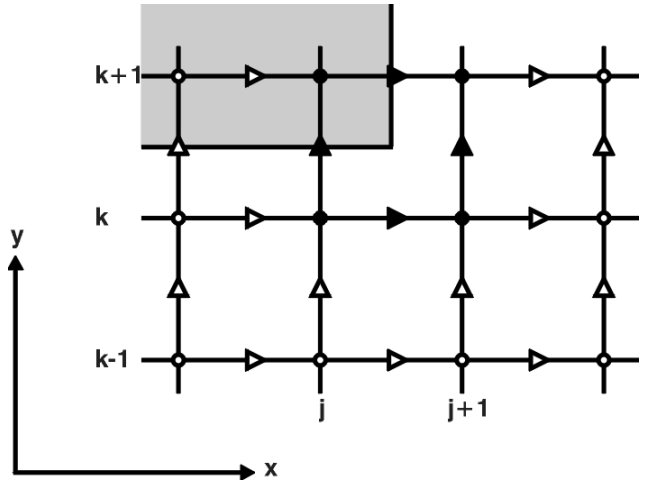

Figure 5.2 Special situations near land. Corner - Exit (CASE 2)

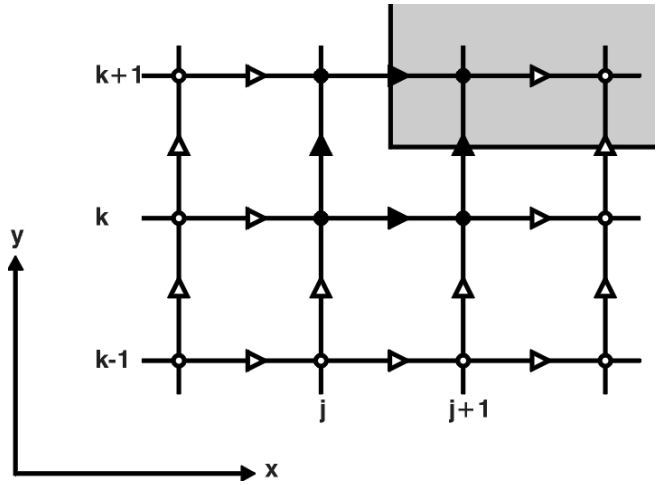

Figure 5.3 Special situations near land. Corner - Entry (CASE 3)

CASE 3: Corner - Entry

Similar assumptions to those in Case 2 give reasonable approximations.

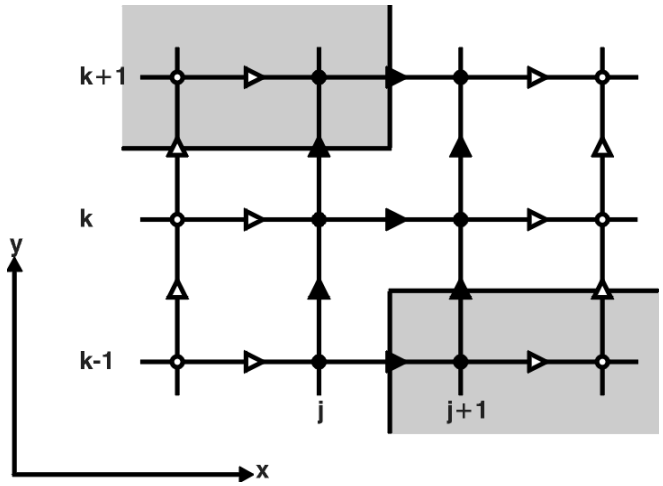

Figure 5.4 Possible corner combination (which should be avoided)

5.2 Shear Terms

The shear terms require an approximation for the cross-derivative terms such as the term $\partial(\nu_T\,\partial u/\partial y)/\partial y$. Consider the general form of this term in (4.24). We have

$$\frac{\partial}{\partial y}\left(\nu_T\frac{\partial u}{\partial y}\right)\approx\left[\frac{\left(u_{k+1}^{n+1}+u_k^n\right)_{j,l}}{\Delta y}\cdot\nu^*_{Tj,k+½,l}-\frac{\left(u_k^{n+1}+u_{k-1}^n\right)_{j,l}}{\Delta y}\cdot\nu^*_{Tj,k-½,l}\right]\frac{1}{\Delta y} \tag{5.4}$$

in which

$$\begin{aligned}\nu^*_{Tj,k+½,l} &= \frac{1}{4}\left(\nu_{Tj,k,l}+\nu_{Tj+1,k,l}+\nu_{Tj,k+1,l}+\nu_{Tj+1,k+1,l}\right)\\ \nu^*_{Tj,k,l+½} &= \frac{1}{4}\left(\nu_{Tj,k,l}+\nu_{Tj+1,k,l}+\nu_{Tj,k,l+1}+\nu_{Tj+1,k,l+1}\right)\end{aligned} \tag{5.5}$$

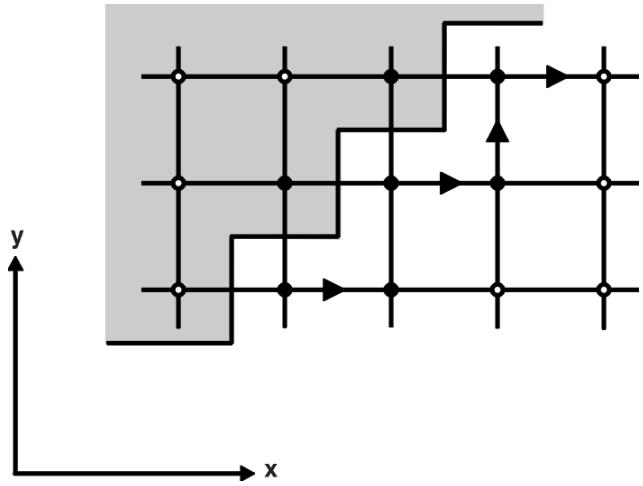

Figure 5.5 Coastline 45° to the grid

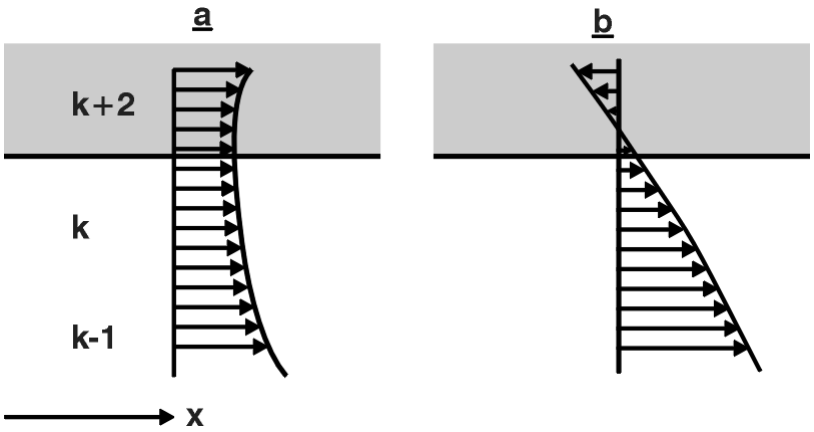

Figure 5.6 Possible velocity distributions

The u_{k+1} and u_{k-1} are approximated using the reflection condition. For Case 1, the ν_T $_{k+1}$'s require an approximation. Experience has shown that the approximation ν_T $_{k+1} \approx \nu_T$ $_k$ in general gives good results. For Case 2, ν_T^* can be approximated as in Case 1. For Case 3 a similar approximation can be applied.

6 Structure of the Difference Scheme, Accuracy, Stability

6.1 Time Centring, Accuracy

The difference schemes developed in the previous section must be seen as one component in a computational cycle. Only together with the other component equations in this cycle is time centring obtained. A full computational cycle is for instance

x-	x-sweep, carried out with decreasing y and z
y-	y-sweep, carried out with decreasing x and z
z-	z-sweep, carried out with decreasing x and y
x+	x-sweep, carried out with increasing y and z
y+	y-sweep, carried out with increasing x and z
z+	z-sweep, carried out with increasing x and y

Referring to a computational cycle we can now discuss the centring of the various terms in the component equations. Consider the (x-) sweep. Its centre is at $n+½$. This is clear for the u terms in the mass equation and the time derivative in the momentum equation. For the time derivative of P, the centring is not obvious. The (x-) sweep itself will not give a centre at $n+½$. The mass equations of the following (y-) and (z-) sweeps have to be involved to provide the centring at $n+½$.

The pressure term in the x-momentum equation is correctly centred at $n+½$.

The spatial derivative for v and w in the mass equations may at first hand appear peculiar. If the centre of the (x-) sweep is at n+½, then why not centre w at n+½ for instance? The explanation lies in the next (y-) and (z-) sweeps. The (y-) sweep has its centre at $n+5/6$ and the mass equation therefore has v at $n+4/3$ and $n+1/3$. Similarly the (z-) sweep has its centre at $n+7/6$ with w at $n+5/3$ and $n+2/3$. Then, when the mass equation of the (y-) and (z-) sweeps are considered together with the mass equation of the (x-) sweep, the v and w terms in the (x-) mass equation are needed to balance the v and w at $n+4/3$ and $n+5/3$, respectively, in the (y-) and (z-) mass equations.

The considerations for the (x-) sweep above can be repeated in a similar manner for the (x+), (y-), (y+), (z-) and (z+) sweeps. Any computational cycle like the shown x-y-z, a y-z-x or a z-x-y will in fact be perfectly time centred at $n+3/6$, $n+5/6$ or $n+7/6$, respectively.

The computational cycle is much similar to the computational cycle employed in MIKE 21 HD. This cycle is described in the *MIKE 21 Scientific Documentation*. Other implicit difference schemes, for example that of Leendertse 1967, are usually based on a closed cycle of similar form.

The difference scheme, by nature of its central difference forms, is generally of second order. It is second order in terms of the discretisation of the Taylor series expansion, as well as in the more classical sense, that of the order of the algorithm. This last concept is defined as the highest degree of a polynomial for which the algorithm is exact. The two definitions are often confused, but they do not necessarily always give the same order of accuracy. For the Laplace equation, the usual central difference approximation is of second order in terms of the discretisation error but the algorithm is of third order. See Leonard 1979.

6.2 Amplification Errors and Phase Errors

6.2.1 General

The finite difference technique is essentially a Taylor series expansion of each of the terms in the partial differential equation under considerations. Such an expansion will lead to an infinite number of functions, which of course cannot be solved numerically as it is fully equivalent to the partial differential equation. The equation is made solvable by discarding the infinite number of functions at a certain level leading to a finite difference equation.

A true solution of a problem represented by the partial differential equation has yet become an approximate solution and the difference between the true solution and the approximate solution is usually denoted the truncation error. It is envisaged that the solutions to the finite difference approximation (or finite difference scheme) will converge towards the true solution of decreasing Δt and Δx. Under such circumstances the finite difference scheme (FDS) is regarded as convergent. It can be shown that if the FDS is stable it will be convergent, too. Thus, the stability of the FDS is a necessary and sufficient condition for convergence.

The relations between Δt and Δx, for which the FDS is stable or unstable, are usually examined through a stability analysis.

A number of features can be considered in a stability analysis such as the phase error, amplification error, numerical vorticity generation, numerical tendency to zigzagging etc. of which the amplification error analysis is probably the most popular one. Here focus is put on the amplification and phase errors.

6.2.2 Theoretical Background

A FDS is called a two-level scheme if it can be expressed on the form

$$\underline{\xi}^{n+1} = \underline{\underline{G}}\ \underline{\xi}^{n} \tag{6.1}$$

Most of the existing FDS'es are of the class given by Equation (6.1) for which a general expression for the phase error has been given by Abbott 1979. As it will be shown in the following, the FDS for MIKE 3 is a three-level scheme for which no similar general expression for the phase error was available and thus, had to be developed; leading to an expression much similar to the expression for the two-level scheme.

Hence, considering any three-level scheme of the form

$$\underline{\xi}^{n+1} = \underline{\underline{A}}\ \underline{\xi}^{n} + \underline{\underline{B}}\ \underline{\xi}^{n-1} \tag{6.2}$$

in which *A* and *B* are arbitrary matrices and ξ a vector containing the prognostic variables. The superscript refers to the time level.

In general, an amplification matrix, *G* multiplying ξ at time level n to give ξ at time level *n+1* may be introduced, i.e.

$$\underline{\underline{\xi}}^{n} = \underline{\underline{G}}_0 \; \underline{\xi}^{n-1} \tag{6.3}$$

$$\underline{\underline{\xi}}^{n+1} = \underline{\underline{G}}_1 \; \underline{\xi}^{n} \tag{6.4}$$

Substituting Equations (6.3) and (6.4) into Equation (6.2) provides the following relation

$$\underline{\underline{G}}_1 = \underline{\underline{A}} + \underline{\underline{B}} \; \underline{\underline{G}}_0^{-1} \tag{6.5}$$

Assuming that

$$\underline{\underline{G}} = \underline{\underline{G}}_0 = \underline{\underline{G}}_1 \tag{6.6}$$

Equations (6.3) and (6.4) yield

$$\underline{\underline{\xi}}^{n+1} = \underline{\underline{G}}^2 \; \underline{\xi}^{n-1} \tag{6.7}$$

Comparing Equation (6.7) with Equation (6.5) shows that the general amplification matrix, *G* is the solution to the equation given by

$$\underline{\underline{G}}^2 - \underline{\underline{A}}\underline{\underline{G}} - \underline{\underline{B}} = 0 \tag{6.8}$$

Clearly, Equation (6.6) must be fulfilled for any stable three-level scheme. Otherwise, any signal of constant form exposed by Equation (6.2) would be amplified under multiplication by G_i. Consequently, Equation (6.7) is equivalent to Equation (6.2) in which *G* is given by Equation (6.8). However, Equation (6.6) does not imply any guarantee for stability; it is only a necessary condition for stability. Thus, the problem is now whether ξ is amplified or whether the amplification is diminishing under multiplication by *G* so that the scheme is stable.

It is well known that the eigenvectors to G do not change under multiplication by *G*. Thus, the corresponding eigenvalues provide an excellent measure for the amplification of ξ. If *X* is an eigenvector of *G* then the corresponding eigenvalue will be a solution to

$$\underline{\underline{G}} \; \underline{X} = g \; \underline{\underline{I}} \; \underline{X} \tag{6.9}$$

where *I* is the identity matrix. For any non-zero eigenvectors Equation (6.9) implies that

$$Det \left| \underline{\underline{G}} - g \; \underline{\underline{I}} \right| = 0 \tag{6.10}$$

Now let the prognostic vector ξ given in Equation (6.2) be exposed by a Fourier transformation in the time domain, i.e.

$$\underline{\xi}^{n} = \sum_k \underline{\xi}_k^{*} e^{-i 2\pi k \delta n \Delta t / l} \tag{6.11}$$

in which k is a dimensionless wave number, δ the celerity given by the differential equation, *n* the time level, Δt the time increment, *l* the wavelength and i the imaginary unit. ξ^* is the corresponding Fourier transformation in the space domain.

Thus, considering any one component of Equation ((6.11) and substituting into Equation (6.2)under the assumption given by Equation (6.6) and rearranging yields

$$\left|\underline{\underline{G}}^2 - e^{-i4\pi k\delta\Delta t/l} \cdot \underline{\underline{I}}\right|\underline{\xi}_k^* = 0 \tag{6.12}$$

from which it follows that

$$(g)^2 = e^{-i4\pi k\delta\Delta t/l} \tag{6.13}$$

In the general case both *g* and δ may be complex. Hence, Equation (6.13) may be re-expressed as

$$\{\mathrm{Re}(g) + i\,\mathrm{Im}(g)\}^2 = \exp\{-i4\pi k(\mathrm{Re}(\delta) + i\,\mathrm{Im}(\delta))\Delta t/l\} \tag{6.14}$$

$$\begin{aligned}&\mathrm{Re}^2(g) - \mathrm{Im}^2(g) + 2i\,\mathrm{Re}(g)\mathrm{Im}(g) = \\ &\exp\{4\pi k\,\mathrm{Im}(\delta)\Delta t/l\}(\cos(4\pi k\,\mathrm{Re}(\delta)\Delta t/l) - i\sin(4\pi k\,\mathrm{Re}(\delta)\Delta t/l))\end{aligned} \tag{6.15}$$

or separating the real and imaginary parts

$$\begin{aligned}&\mathrm{Re}^2(g) - \mathrm{Im}^2(g) = \\ &\exp\{4\pi k\,\mathrm{Im}(\delta)\Delta t/l\}\cdot\cos\{4\pi k\,\mathrm{Re}(\delta)\Delta t/l\}\end{aligned} \tag{6.16}$$

$$\begin{aligned}&2\,\mathrm{Re}(g)\mathrm{Im}(g) = \\ &-\exp\{4\pi k\,\mathrm{Im}(\delta)\Delta t/l\}\cdot\sin\{4\pi k\,\mathrm{Re}(\delta)\Delta t/l\}\end{aligned} \tag{6.17}$$

Following the work of Leendertse 1967 and Vliegenthart 1968 a complex propagation factor defined in terms of the wave numbers may be introduced

$$P = P(k) = \frac{e^{i2\pi k(x-\delta t)/l}}{e^{i2\pi k(x-\lambda t)/l}} \tag{6.18}$$

in which λ is the celerity given by the FD equation. Following *P* over a time interval in which the component of wave number k propagates over its entire wavelength gives

$$P = e^{-i2\pi(\delta/\lambda - 1)} \tag{6.19}$$

The argument of *P*, which provides a measure for the phase error, reads

$$Arg\ P = 2\pi \left\{ 1 - \frac{\mathrm{Re}(\delta)}{\lambda} \right\} \tag{6.20}$$

For convenience, the phase error is expressed in terms of a celerity ratio, Q, defined by

$$Q = \frac{\mathrm{Re}(\delta)}{\lambda} \tag{6.21}$$

Eliminating the imaginary part of δ from Equation (6.15) and substituting into Equation (6.19) yields after some algebra

$$Q = \frac{1}{4\pi k\lambda \Delta t / l} \cdot \mathrm{Arctan}\left\{ \frac{2\,\mathrm{Re}(g)\mathrm{Im}(g)}{\mathrm{Re}^2(g) - \mathrm{Im}^2(g)} \right\} \tag{6.22}$$

Introducing the Courant number defined as

$$C_{rs} = \lambda \frac{\Delta t}{\Delta s} \tag{6.23}$$

where Δs is the grid spacing in the s-direction, Equation (6.20) may be rearranged to yield

$$Q = -\frac{N_s}{4\pi C_{rs}} \cdot \mathrm{Arctan}\left\{ \frac{2\,\mathrm{Re}(g)\mathrm{Im}(g)}{\mathrm{Re}^2(g) - \mathrm{Im}^2(g)} \right\} \tag{6.24}$$

in which N_s is the number of computational points per wavelength.

Equation (6.22) is much similar to the equivalent expression for a two-level scheme (see Abbott 1979).

Thus, the phase error of any three-level scheme is expressed through Equation (6.22) whereas the amplification error is expressed through the modulus of the set of eigenvalues. For any unstable schemes the modulus will be greater than unity whereas any dissipative scheme will have eigenvalues smaller than unity. It can be shown that the necessary condition $|g| \le 1$ is also a sufficient condition for stability (see Abbott 1979).

6.2.3 Characteristics of MIKE 3

The characterisation of the MIKE 3 scheme through the phase and amplification properties is based on the most simple case, which is neglecting effects of advection, viscosity, stratification etc. Doing so, the basic equations are reduced to

$$\frac{1}{\rho c_s^2}\frac{\partial P}{\partial t} + \frac{\partial u_j}{\partial x_j} = 0 \tag{6.25}$$

$$\frac{\partial u_i}{\partial t} + \frac{1}{\rho}\frac{\partial P}{\partial x_i} = 0 \tag{6.26}$$

Notice that the gravity term has been omitted in Equation (6.24). We will revert to this later in Section 9. The three mass equations are given by Equations (4.2) to (4.4). The finite difference approximations of the momentum equations read

$$\frac{u_{j,k,l}^{n+1}-u_{j,k,l}^{n}}{\Delta t}+\frac{1}{\rho}\frac{P_{j,k,l}^{n+\frac{1}{2}}-P_{j-1,k,l}^{n+\frac{1}{2}}}{\Delta x}=0 \tag{6.27}$$

$$\frac{v_{j,k,l}^{n+\frac{4}{3}}-v_{j,k,l}^{n+\frac{1}{3}}}{\Delta t}+\frac{1}{\rho}\frac{P_{j,k,l}^{n+\frac{5}{6}}-P_{j,k-1,l}^{n+\frac{5}{6}}}{\Delta y}=0 \tag{6.28}$$

$$\frac{w_{j,k,l}^{n+\frac{5}{3}}-w_{j,k,l}^{n+\frac{2}{3}}}{\Delta t}+\frac{1}{\rho}\frac{P_{j,k,l}^{n+\frac{7}{6}}-P_{j,k,l-1}^{n+\frac{7}{6}}}{\Delta z}=0 \tag{6.29}$$

For each of the prognostic variables a Fourier transformation in the space domain given by

$$\xi_{j,k,l}^{n}=\sum_{m}\xi_{*}^{n}\cdot\exp\left(im2\pi j\Delta x/l_{wave}\right)\cdot\exp\left(im2\pi k\Delta y/l_{wave}\right)\cdot\exp\left(im2\pi l\Delta z/l_{wave}\right) \tag{6.30}$$

is introduced, whereby Equations (6.25) to (6.27) may be expressed in terms of a set of Fourier transformations. Now, consider any one component of Equation (6.28) and recall that

$$\left\{\ e^{i\psi}-e^{-i\psi}\ \right\}\ =\ 2i\sin(\psi) \tag{6.31}$$

For convenience three dimensionless variables are introduced, defined by

$$\alpha\ =\ \frac{2}{3}\ \frac{c_s\Delta t}{\Delta x}\ \sin\ \left(\frac{\pi}{N_x}\right)$$

$$\beta\ =\ \frac{2}{3}\ \frac{c_s\Delta t}{\Delta y}\ \sin\ \left(\frac{\pi}{N_y}\right) \tag{6.32}$$

$$\gamma\ =\ \frac{2}{3}\ \frac{c_s\Delta t}{\Delta z}\ \sin\ \left(\frac{\pi}{N_z}\right)$$

Substituting Equations (6.28) to (6.30) into Equations (6.25) to (6.27) and eliminating all pressure terms provide after some algebra the following three equations:

$$\left(1+\alpha^2\right)\ u_*^{n+1} = -\left(1-\alpha^2\right)\ u_*^n - \alpha^2\left(\beta - \frac{1}{\beta}\right)\ v_*^{n+\frac{1}{3}}$$

$$\alpha\gamma\ \ w_{w*}^{n+\frac{2}{3}} - \alpha\left(\beta - \frac{1}{\beta}\right)\ v_*^{n-\frac{2}{3}} - \alpha\gamma\ \ w_*^{n-\frac{1}{3}} \tag{6.33}$$

$$\left(1+\beta^2\right)\ v_*^{n+\frac{4}{3}} + \alpha\beta\ \ u_*^{n+1} = -\alpha\,\beta\,u_*^n$$

$$-\left(1-\beta^2\right)\ v_*^{n+\frac{1}{3}} + \beta\left(\gamma - \frac{1}{\gamma}\right)\ \ w_*^{n+\frac{2}{3}} - \beta\left(\gamma + \frac{1}{\gamma}\right)\ \ w_*^{n-\frac{1}{3}} \tag{6.34}$$

$$\left(1+\gamma^2\right)\ w_*^{n+\frac{5}{6}} + \gamma\beta\ \ v_*^{n+\frac{4}{3}} + \gamma\left(\alpha - \frac{1}{\alpha}\right)\ \ u_*^{n+1} =$$
$$-\gamma\left(\alpha + \frac{1}{\alpha}\right)\ \ u_*^n - \beta\gamma\ \ v_*^{n+\frac{1}{3}} + \left(1-\gamma^2\right)\ \ w_*^{n+\frac{2}{3}} \tag{6.35}$$

On matrix form Equations (6.31) to (6.33) read

$$\begin{bmatrix} 1+\alpha^2 & 0 & 0 \\ \alpha\beta & 1+\beta^2 & 0 \\ \gamma\left(\alpha - \frac{1}{\alpha}\right) & \gamma\beta & 1+\gamma^2 \end{bmatrix} \begin{bmatrix} u_*^{n+1} \\ v_*^{n+\frac{4}{3}} \\ w_*^{n+\frac{5}{3}} \end{bmatrix} =$$

$$\begin{bmatrix} 1-\alpha^2 & -\alpha\left(\beta - \frac{1}{\beta}\right) & -\alpha\gamma \\ -\alpha\beta & 1-\beta^2 & -\beta\left(\gamma - \frac{1}{\gamma}\right) \\ -\gamma\left(\alpha - \frac{1}{\alpha}\right) & -\gamma\beta & 1-\gamma^2 \end{bmatrix} \begin{bmatrix} u_*^{n-1} \\ v_*^{n+\frac{1}{3}} \\ w_*^{n-\frac{1}{3}} \end{bmatrix} + \tag{6.36}$$

$$\begin{bmatrix} 0 & -\alpha\left(\beta + \frac{1}{\beta}\right) & -\alpha\gamma \\ 0 & 0 & -\beta\left(\gamma + \frac{1}{\gamma}\right) \\ 0 & 0 & 0 \end{bmatrix} \begin{bmatrix} u_*^{n-1} \\ v_*^{n-\frac{2}{3}} \\ w_*^{n-\frac{1}{3}} \end{bmatrix}$$

Comparing Equation (6.34) with Equation (6.2) shows that the MIKE 3 FDS forms a three-level scheme of the type given by Equation (6.2)in which

$$\underline{\xi}^n = \left[u_*^n, v_*^{n+\frac{1}{3}}, w_*^{n+\frac{2}{3}} \right]^T \tag{6.37}$$

The Fourier coefficient ξ_*^n is now extended to the time domain as

$$\xi_*^n = \xi * \cdot e^{i\omega\Delta t} = \xi * \cdot \phi \tag{6.38}$$

such that ϕ itself is the amplification factor over the time Δt. Substituting Equation (6.36) into Equation (6.34) yields after some algebra

$$\begin{bmatrix} \phi^2\left(\alpha+\frac{1}{\alpha}\right)+\phi\left(\alpha-\frac{1}{\alpha}\right) & \phi\left(\beta-\frac{1}{\beta}\right)+\left(\beta+\frac{1}{\beta}\right) & \phi\gamma+\gamma \\ \phi^2\alpha+\phi\alpha & \phi^2\left(\beta+\frac{1}{\beta}\right)+\phi\left(\beta-\frac{1}{\beta}\right) & \phi\left(\gamma-\frac{1}{\gamma}\right)+\left(\gamma+\frac{1}{\gamma}\right) \\ \phi^2\left(\alpha-\frac{1}{\alpha}\right)+\phi\left(\alpha+\frac{1}{\alpha}\right) & \phi^2\beta+\phi\beta & \phi^2\left(\gamma+\frac{1}{\gamma}\right)+\phi\left(\gamma-\frac{1}{\gamma}\right) \end{bmatrix} \cdot \xi_* = 0 \tag{6.39}$$

Solving Equation (6.37) with respect to ϕ yields the following equation of fourth order

$$A\phi^4 + B\phi^3 - B\phi - A = 0 \tag{6.40}$$

where

$$A = \left(1+\alpha^2\right)\left(1+\beta^2\right)\left(1+\gamma^2\right)$$

$$B = 2\left(1+\alpha^2\right)\left(1+\beta^2\right)\left(1+\gamma^2\right) - \left(1+\alpha^2\right)\left(1+\beta^2\right) - \left(1+\gamma^2\right) - 1 \tag{6.41}$$

Equation (6.38) can be decomposed into

$$(\phi+1)(\phi-1)\left(A\phi^2+B\phi+A\right) = 0 \tag{6.42}$$

of which the last bracket has the solutions

$$\phi = -\frac{B}{2A} \pm i\frac{D}{2A} \tag{6.43}$$

where

$$D^2 = 4A^2 - B^2, D \in R^+ \tag{6.44}$$

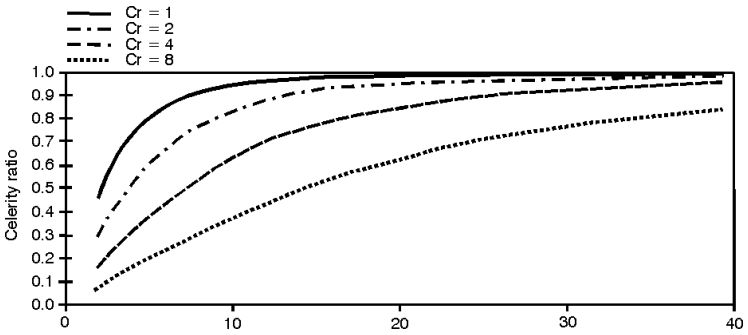

Figure 6.1 Phase portrait for flow propagating along a grid line

From Equations (6.40) and (6.41) it is seen that the amplification factor moduli are always one for all ϕ. Hence, the FDS in the form of Equations (6.23) to (6.24) is unconditionally stable. Substituting the two real solutions into Equation (6.22) implies a celerity ratio zero or no phase error.

For the two complex solutions phase portraits can be established for various Courant numbers, and flow directions. A typical example on a phase portrait for a flow propagating along a grid line has been shown in Figure 6.1. It is seen that for a Courant number of one, approximately 20 points per wavelength are needed (and increasing with the Courant number) in order to obtain the correct physical celerity of the flow.

7 Lateral Boundary Conditions

7.1 General

The main purpose of hydrodynamic module of MIKE 3 is to solve the partial differential equations that govern three-dimensional flow. Like all other differential equations they need boundary conditions. The importance of boundary conditions cannot be overstressed.

In general the following boundary data are needed:

- Pressure (or surface level) at the open boundaries and velocities parallel to the open boundaries

  or

- Velocities both perpendicular and parallel to the open boundaries
- Bathymetry (depths and land boundaries)
- Bed resistance
- Wind speed, direction and shear coefficient
- Barometric pressure (gradients)

The success of a particular application of MIKE 3 is dependent upon a proper choice of open boundaries more than on anything else. The factors influencing the choice of open boundaries can roughly be divided into two groups, namely

- Grid-derived considerations
- Physical considerations

The physical considerations concern the area to be modelled and the most reasonable orientation of the grid to fit the data available and will not be discussed further here.

The grid itself implies that the open boundaries must be positioned parallel to one of the coordinate axes. (This is not a fundamental property of a finite difference scheme but it is essential when using MIKE 3).

Furthermore, the best results can be expected when the flow is approximately perpendicular to the boundary. This requirement may already be in contradiction with the above mentioned grid requirements, and may also be in contradiction with "nature" in the sense that flow directions at the boundary can be highly variable so that, for instance "360" flow directions occur, in which case the boundary is a most unfortunate choice.

7.2 Primary Open Boundary Conditions

The primary boundary conditions can be defined as the boundary conditions sufficient and necessary to solve the linearised equations. The fully linearised x-momentum equation reads:

$$\frac{\partial u}{\partial t} + \frac{1}{\rho}\frac{\partial P}{\partial x} = 0 \tag{7.1}$$

The corresponding terms in the x-momentum equation of MIKE 3 are:

$$\frac{\partial u}{\partial t} + \cdots + \frac{1}{\rho}\frac{\partial P}{\partial x} + \cdots = 0 \tag{7.2}$$

A "**dynamic case**" we define as a case where

$$\frac{\partial u}{\partial t} \approx -\frac{1}{\rho}\frac{\partial P}{\partial x} \tag{7.3}$$

i.e. a case where these two terms dominate over all other terms of the x-momentum equation.

It is then clear that the primary boundary conditions provide "almost all" the boundary information necessary for the hydrodynamic module of MIKE 3 when it is applied to a dynamic case. The same set of boundary conditions maintain the dominant influence (but are in themselves not sufficient) even in the opposite of the "dynamic case", namely the steady state (where the linearised equations are quite meaningless). This explains why these boundary conditions are called "primary".

MIKE 3 accepts two basic types of primary boundary conditions:

- Pressure (or surface elevation)
- Velocities

They must be given at all boundary points and at all time steps.

It should be mentioned that - due to the space staggered scheme - the values of the velocities at the boundary are set half a grid point **inside** the topographical boundary, see Figure 7.1.

7.3 Secondary Open Boundary Conditions

7.3.1 General

The necessity for secondary boundary conditions arises because one cannot close the solution algorithm at **open** boundaries when using the non-linearised equations. Additional information has to be given and there are several ways to give this. The hydrodynamic module of MIKE 3 is built on the premise that the information missing is **the horizontal velocities parallel to the open boundary and the vertical velocities are negligible**.

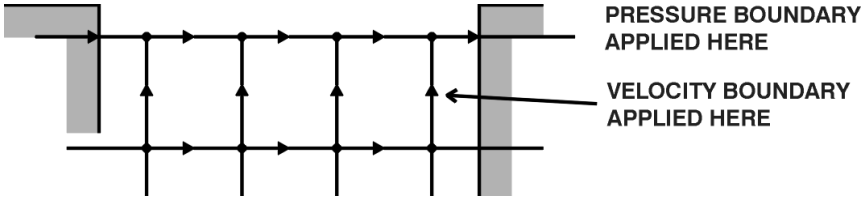

Figure 7.1 Application of boundary data at a northern boundary

This is chosen because it coincides conveniently with the fact that the simplified MIKE 3 hydrodynamic model - the model that is one-dimensional in the horizontal space - does not require a secondary boundary condition (i.e. the velocities parallel to the boundary are zero).

As a consequence of the transport character of the convective terms, a "true" secondary condition is needed at inflows, whereas at outflow a "harmless" closing of the algorithm is required. This closing may either be obtained by defining the flow at the boundary or by extrapolation of the velocities along the boundary from the interior. Furthermore, the velocities outside the boundaries are needed (for the convective and shear terms in the momentum equations.

7.4 Wind Friction

The wind friction originates from the vertical shear term assuming a balance between the wind shear and the water shear at the surface

$$\frac{\tau_{xz}}{\rho} = \nu_T \frac{\partial u}{\partial z} = \frac{\rho_{air}}{\rho} C_w W W_x \tag{7.4}$$

where ρ_{air} is the density of air, W the wind speed and C_W the wind drag coefficient. The wind friction is thus a boundary condition to vertical shear term. The wind friction factor is calculated in accordance with Smith & Banke 1975, see Figure 7.2.

$$C_w = \begin{cases} C_{w0} & for \quad W < W_0 \\ C_{w0} + \dfrac{W - W_0}{W_1 - W_0} \cdot (C_{w1} - C_{w0}) & for \quad W_0 \le W \le W_1 \\ C_{w1} & for \quad W > W_1 \end{cases} \tag{7.5}$$

where

$$\begin{aligned} C_{w0} &= 0.0013, \; W_0 = 0 \; m/s \\ C_{w1} &= 0.0026, \; W_1 = 24 \; m/s \end{aligned} \tag{7.6}$$

7.4.1 Bed Resistance

Similar to the wind friction the bed resistance originates from the vertical shear term as a boundary condition. In MIKE 3 a logarithmic velocity profile is assumed between the actual seabed and first computational node encountered above (except for the Smagorinsky eddy viscosity formulation),

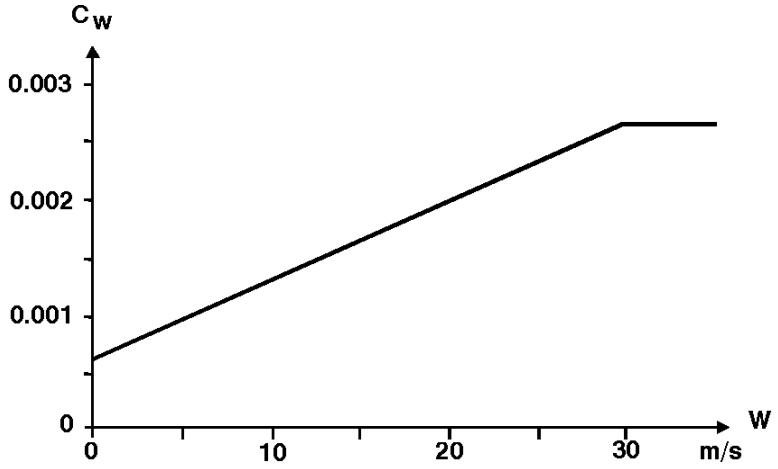

Figure 7.2 Wind friction factor

$$\frac{\tau_{xz}}{\rho} = \nu_T \frac{\partial u}{\partial z} = \left[\frac{1}{\kappa} \log\left(\frac{z_b}{k_s/30} \right) \right]^{-2} \cdot U(z_b) \cdot u(z_b) \tag{7.7}$$

in which κ is von Kármán's constant, k_s the bed roughness, U the current speed, u is the current velocity and z_b the distance above the seabed.

If the Smagorinsky eddy viscosity formulation is applied then a slightly different formulation is used such that the drag coefficient formulation is consistent with the turbulence closure model. In this case, the shear stress is given by the relation

$$\frac{\tau_{xz}}{\rho} = \nu_T \frac{\partial u}{\partial z}$$

$$= \left[\frac{2\sqrt{2}}{3} \frac{D}{l} \left\{ \left(1 - \frac{z_m}{D} \right)^{\frac{3}{2}} - \left(1 - \frac{z_b}{D} \right)^{\frac{3}{2}} \right\} + \frac{1}{\kappa} \log\left(\frac{z_m}{k_S/30} \right) \right]^{-2} \cdot U(z_b) \cdot u(z_b) \tag{7.8}$$

where z_m is the distance above the seabed where the Smagorinsky velocity profile matches the logarithmic profile, l is the Smagorinsky length scale and D the water depth.

8 Boundary Conditions for the Vertical Sweep

In the design of MIKE 3 main focus has been put on free surface flows but MIKE 3 can also handle flow problems with rigid lids. Due to the artificial compressibility method, however, some precaution should be taken in applications involving rigid lids. In these situations the upper boundary condition for the z sweep is similar to the ones used in the horizontal direction at land boundaries i.e. the velocity perpendicular to the land boundary is identical to zero. This is also the boundary condition used at the seabed in the z sweeps. Accordingly, only the case of free surface flows needs to be considered here.

The free surface constitutes a special case as it can be regarded as a moving boundary. In MIKE 3 the kinematic boundary condition is used which reads

$$w_\eta = \frac{D\eta}{Dt} \tag{8.1}$$

in which η is the surface elevation relative to the datum level. The relations given by Equation (3.3) require a relationship between the kinematic boundary condition and the fluid pressure at the first computational point encountered from the surface and downwards. The simplest relation is the hydrostatic pressure assumption whereby η is related to P according to

$$P(z) = \rho g(\eta + z) \tag{8.2}$$

Thus between the actual surface and the first node MIKE 3 applies a hydrostatic pressure assumption. The convective term $\partial w/\partial z$ as well as the shear term $\partial(2\nu_T\, \partial w/\partial z)/\partial z$ requires information about the vertical velocity at the top level. To determine this we use a reflection boundary condition,

$$\left.\frac{\partial w_\eta}{\partial z}\right|_\eta = 0 \tag{8.3}$$

As it virtually is $w_{j,k,l+½}$ and not w_η which is required in the finite difference approximations Equation (8.3) is coupled to $w_{j,k,l+½}$ using a second order interpolation (or extrapolation),

$$\begin{aligned} w_\eta &= \Lambda w_{l+½} + (1-\Lambda) w_{l-½} \\ \Lambda &= \frac{\left(\eta + \frac{3}{2}\Delta z\right)^2}{2\Delta z(\eta + \Delta z)} \end{aligned} \tag{8.4}$$

The coefficients in Equation (3.2) can hereby be determined and the z sweep be solved in the usual manner.

9 Definition of Excess Pressure

Implementation of Equation (2.2) directly would imply a large fluid pressure due to the hydrostatic pressure. In order to prevent flow caused by computer round-off errors, which may occur in simulations with large depths, an excess pressure, P^*, is introduced defined by

$$P^* = P - \rho g z \tag{9.1}$$

Moreover, Equation (9.1) provides any variation in the density, ρ to be expressed explicitly in accordance with the separation of the prognostic variables in the hydrodynamics and advection-dispersion modules. It is emphasised that ρ in Equation (9.1) is the local density and not a reference density whereby Equation (9.1) would equal the Boussinesq approximation.

Substituting Equation (9.1) into the pressure derivative of Equation (2.2)yields

$$\frac{1}{\rho}\frac{\partial P}{\partial x_i} = \frac{1}{\rho}\frac{\partial P^*}{\partial x_i} + \frac{gz}{\rho}\frac{\partial \rho}{\partial x_i} + g\frac{\partial z}{\partial x_i} \tag{9.2}$$

from which it is seen that the gravity term in Equation (2.2) vanishes by this definition. Instead an additional space derivative term with respect to ρ has been introduced. This will, however, vanish for homogeneous fluids.

A similar operation can be applied to the mass equation given by Equation (2.1) using the equation of state to convert the time derivative of ρ back into a pressure time derivative. This implies a minor modification of the compressibility. However, as we always use an artificial compressibility there in no need to take this into account. It can conveniently be considered as embedded in the artificial compressibility.

The adoption of the excess pressure definition requires a special, initial excess pressure distribution for inhomogeneous fluids. As initial condition, a balance between the excess pressure and the density variation is assumed, i.e.

$$P^*(z) = -\rho g z + g\int_z \rho dz \tag{9.3}$$

For homogeneous fluids Equation (9.3) will equal zero.

The introduction of an excess pressure is solely done because it is more convenient from a numerical point of view, and does not have any effect on the other terms apart from those mentioned here. However, in stratified simulations it can sometimes be a little difficult to interpret the pressure in a classical manner, because of the special density dependency.

10 Fundamental Aspects of Three-Dimensional Modelling

10.1 General

As mentioned in Section 2, the divergence-free mass equation together with the momentum equations mathematically form an ill-conditioned problem because the fluid pressure does not appear in the divergence-free mass equation, which causes a weak coupling between the pressure and the velocities. **This is the key issue in three-dimensional modelling**. The system is said to be stiff as both slow and fast processes are present which inherently cause difficulties in numerical algorithms. Mathematically this implies zeros in the main diagonal of M in Equation (3.1). The solution of Equation (3.1) inherently requires iteration and that even with a slow convergence. Fortunately different ways to overcome this drawback have been devised. These can all be grouped into three fundamental classes (see e.g. Rasmussen 1993),

- pressure eliminating methods
- pressure correcting methods
- artificial compressibility methods

The three classes are briefly discussed in the following sections.

10.2 Pressure Eliminating Methods

The first class comprises methods, which will eliminate the pressure from the momentum equations. The most commonly used method of this class is the hydrostatic assumption whereby the pressure can be replaced by information about the surface elevation. The technique is well known and accordingly need not to be discussed further. In two-dimensional modelling the definition of a vorticity is often used to eliminate the pressure. This technique is also applicable in three-dimensional modelling. However, the set of equations becomes more complicated compared to its two-dimensional counterpart because three vorticities are required whereas only one is needed in two dimensions. Therefore it is rarely used in three dimensions.

10.3 Pressure Correcting Methods

The second class comprises methods, which correct the pressure to obtain a divergence-free mass equation. It differs fundamentally from the first class by retaining the pressure as one of the prognostic variables. The divergence-free continuity equation is enforced through the solution of a Poisson equation for the pressure (see e.g. Ferziger 1987, Patankar 1980). The Poisson equation is derived by taking the divergence of the momentum equations and applying the divergence-free mass equation. However, in most models where this technique is applied the viscosity is assumed constant. The expression is no longer simple if this assumption is not made and it becomes even more complicated if a variable density is considered. Despite the fact that the solution of the Poisson equation is not a straightforward task from a numerical point of view it has been very popular and is probably the most commonly used method amongst those which retain the pressure as a prognostic variable.

10.4 Artificial Compressibility Methods

In free surface flows only the slow processes are of interest and usually the fast processes (like shock waves) have no substantial influence on the slow processes (like the free surface waves) suggesting that they may be removed without loss of information. The fast processes are easily eliminated by replacing the time derivative of the density in the mass conservation equation with the pressure term in the equation of state, whereby a compressibility of the fluid is introduced. The fast processes are then subsequently eliminated through an artificial compressibility whereby the system mathematically has become hyperbolically dominated. This allows for efficient solution techniques to be adopted. This approach is known as the artificial compressibility approach and was first proposed by Chorin 1967.

Theoretically the physical compressibility of seawater may be used which would make the mass equation valid from a physical point of view. However, this would imply an impractical restriction on the time step, which in turn would exclude any practical application.

10.5 The Compressibility in MIKE 3

It is the artificial compressibility method, which has been adopted in the non-hydrostatic version of MIKE 3. The reason for this is not that it is believed to be superior to any of the other methods. It is entirely because it allows the same solution technique as used in most of DHI's other modelling systems including the MIKE 21 and with which DHI has many years of experience.

It is well known that artificial compressibility is an excellent tool to enforce a faster convergence in steady state simulations. On the other hand, it is certainly not obvious that the same technique can be applied in highly dynamic simulations too. However, many experiments and applications have in fact shown that this is the case provided that the artificial compressibility is chosen with some care. It is evident that for instance the compressibility must not become less than the celerity of the free surface waves. In the hydrostatic version of MIKE 3 the compressibility is a function of the grid spacing, time step and the maximum water depth,

$$c_s = \pi^4 \sqrt{g \; h_{\max} \left(\frac{\Delta x}{\Delta t} \right)^2} \tag{10.1}$$

where h_{max} is the maximum water depth in the model area. There is - so far - no scientific argument for (10.1) except that it appears to give good results. Fortunately experiments have shown that the range of c_s-values which will give the correct physical wave propagation is rather broad.

If the compressibility is too high the system will become stiff (the pressure information travels fast) whereby the model will have difficulties in spreading the information to its surroundings through the convective terms and shear terms. The solution consequently tends to reflect the characteristics of the adopted non-iterative ADI algorithm. On the other hand, if the compressibility is too low the system becomes like jelly and the flow will not propagate will the correct physical celerity. The basic philosophy is that the compressibility should be chosen such that neither of these cases occurs.

Furthermore, in free surface flows the z sweep will release whatever of pressure that has been accumulated during the x and y sweeps such that the surface elevation is adjusted. Experience has shown that the non-hydrostatic version MIKE 3 also does well in applications with limited rigid lids such as floating breakwaters and ships as the pressure underneath

floating bodies essentially is governed by the surrounding pressure field. If no free surface is present the non-hydrostatic version of MIKE 3 should only be used for steady state applications unless the time step is accordingly decreased.

11 Description of the Bottom-Fitted Approach

11.1 General

Bottom-fitted coordinates are defined as being coordinates, which take into account the actual depths. The bottom-fitted coordinates are only applied at the lowermost level that is to say the "standard definitions" are applied above the lowermost computational nodes. This approach differs from the σ coordinate system, which also is bottom-fitted in the way that the bathymetry in the σ coordinate system affects the thickness of all layers. In the approach used in MIKE 3, the vertical grid spacing will be Δz above the lowermost computational nodes (except for the surface layer) whereas the "control volume" for the lowermost computational nodes will vary to fit the actual depth.

11.2 Mathematical Background

11.2.1 Conservation of mass

Averaging the equation for conservation of mass, Equation (2.1) from the seabed to $½\Delta z$ over the first computational node yields,

$$\frac{1}{\gamma + ½\Delta z}\int_{-\gamma}^{½\Delta z}\left(\frac{1}{\rho c_s^2}+\frac{\partial u}{\partial x}+\frac{\partial v}{\partial y}+\frac{\partial w}{\partial z}=SS\right)dz \tag{11.1}$$

where γ is defined being the distance from the actual seabed to the first computational node encountered. On conservation form Equation (11.1)can be rearranged to yield,

$$\frac{1}{\rho_s^2}\frac{\partial P}{\partial t}+\frac{1}{\gamma + ½\Delta z}\left(\frac{\partial \int_{-\gamma}^{½\Delta z} u dz}{\partial x}+\frac{\partial \int_{-\gamma}^{½\Delta z} v dz}{\partial y}+w\Big|_{½\Delta z}\right)=SS \tag{11.2}$$

It is important to keep Equation (11.2) on conservation form instead of Eulerian form on which the averaging will have no effect except for the vertical term.

11.2.2 Conservation of momentum

Applying the same averaging technique as for the mass equation the momentum equations in Equation (2.2) yield,

$$\frac{\partial u_i}{\partial t} + \frac{1}{\gamma + ½\Delta z}\frac{\partial \int_{-\gamma}^{½\Delta z} u_i u_j dz}{\partial x_j} + 2\Omega_{ij} u_j = -\frac{1}{\rho}\frac{\partial P}{\partial x_i} - \frac{gz}{\rho}\frac{\partial \rho}{\partial x_i}$$

$$+ \frac{1}{\gamma + ½\Delta z}\frac{\partial}{\partial x_j}\left(v_T \left(\frac{\partial \int_{-\gamma}^{½\Delta z} u_i dz}{\partial x_j} + \frac{\partial \int_{-\gamma}^{½\Delta z} u_j dz}{\partial x_i} \right) - \frac{2}{3}\delta_{ij} \int_{-\gamma}^{½\Delta z} k dz \right) + u_i SS \tag{11.3}$$

It is stressed that neither the excess pressure term nor the density term is affected by the averaging. Similar to the mass equation the discretised form of Equation (11.3) will depend on whether an Eulerian or a conservation formulation is applied.

11.2.3 Conservation of a scalar quantity

In simulations in stratified areas or in water quality and eutrophication simulations a general transport equation is solved in addition to the mass and momentum equations. The general transport equation for a scalar quantity reads,

$$\frac{\partial C}{\partial t} + \frac{\partial (u_j C)}{\partial x_j} = \frac{\partial}{\partial x_j}\left(D_j \frac{\partial C}{\partial x_j} \right) + SS \tag{11.4}$$

in which C denotes the scalar quantity and D_j the dispersion coefficient. Averaging this equation yields,

$$\frac{\partial C}{\partial t} + \frac{1}{\gamma + ½\Delta z}\left(\frac{\partial \int_{-\gamma}^{½\Delta z} (uC) dz}{\partial x} + \frac{\partial \int_{-\gamma}^{½\Delta z} (vC) dz}{\partial y} + (wC)\big|_{½\Delta z} \right) =$$

$$\frac{1}{\gamma + ½\Delta z}\left(\frac{\partial}{\partial x}\left(D_x \frac{\partial \int_{-\gamma}^{½\Delta z} C dz}{\partial x} \right) + \frac{\partial}{\partial y}\left(D_y \frac{\partial \int_{-\gamma}^{½\Delta z} C dz}{\partial y} \right) + + D_Z \frac{\partial C}{\partial z}\Big|_{½\Delta z} \right) + SS \tag{11.5}$$

11.3 Numerical Implementation

11.3.1 Conservation of Mass

The numerical implementation of the bottom-fitted coordinates is done with due respect to the original implementation in MIKE 3. Hence, using the standard notation from MIKE 3 the finite difference form the spatial discretisation of Equation (11.2) reads,

$$\frac{1}{\rho c_s^2}\frac{\Delta P_{j,k,l}}{\Delta t}+\frac{u_{j,k,l}\bar{\gamma}^*_{j,k,l}-u_{j,k,l}\bar{\gamma}^*_{j-1,k,l}}{\gamma^*_{j,k,l}\Delta x} \tag{11.6}$$

$$+\frac{v_{j,k,l}\bar{\gamma}^*_{j,k,l}-v_{j,k-1,l}\bar{\gamma}^*_{j,k-1,l}}{\gamma^*_{j,k,l}\Delta y}+\frac{w_{j,k,l}}{\gamma^*_{j,k,l}}=SS$$

in which γ^* denotes the distance from the actual seabed to ½Δz over the first computational node above. The overbar refers to correct spatial centred values. Equation (11.6) can be further rearranged to read,

$$\frac{1}{\rho c_s^2}\frac{\Delta P_{j,k,l}}{\Delta t}+\frac{u_{j,k,l}\dfrac{\bar{\gamma}^*_{j,k,l}}{\gamma^*_{j,k,l}}-u_{j-1,k,l}\dfrac{\bar{\gamma}^*_{j-1,k,l}}{\gamma^*_{j,k,l}}}{\Delta x} \tag{11.7}$$

$$+\frac{v_{j,k,l}\dfrac{\bar{\gamma}^*_{j,k,l}}{\gamma^*_{j,k,l}}-v_{j,k-1,l}\dfrac{\bar{\gamma}^*_{j,k-1,l}}{\gamma^*_{j,k,l}}}{\Delta y}+\frac{w_{j,k,l}\dfrac{\Delta z}{\gamma^*_{j,k,l}}-w_\gamma(\equiv 0)\dfrac{\Delta z}{\gamma^*_{j,k,l}}}{\Delta z}=SS$$

Thus, near the bottom the velocities are adjusted according to the heights of the control volumes. $\bar{\gamma}^*$ is different for the x- and y-direction due to the spatial centring of the velocities. In principle only one extra two-dimensional array is required but as the $\bar{\gamma}^*$'s are constant throughout the simulation it may be advantageously to calculate these quantities once on the account of extra memory.

11.3.2 Conservation of Momentum

To be consistent with the present discretisation in MIKE 3 the conservation form is adopted. In general the averaging technique inevitably implies that the discretised convective and eddy terms will be off-centred when imposed on the C-grid. Numerically this implies that the accuracy of these terms go down from 2nd order to 1st order. Correction terms may, however, be implemented to bring the accuracy up again. As a first approach a 1st order accuracy on these terms is accepted.

The affected terms are handled separately for each of the three momentum equations. The averaging procedure for the x-momentum yields,

$$FDS\left(\frac{1}{\gamma+½\Delta z}\frac{\partial\int_{-\gamma}^{½\Delta z}(uu)dz}{\partial x}\right)=$$

$$\frac{\frac{\gamma^*_{j+1,k,l}}{\bar{\gamma}^*_{j,k,l}}\left(u_{j+1,k,l}+u_{j,k,l}\right)^2-\frac{\gamma^*_{j,k,l}}{\bar{\gamma}^*_{j,k,l}}\left(u_{j,k,l}+u_{j-1,k,l}\right)^2}{4\Delta x}$$

$$FDS\left(\frac{1}{\gamma+½\Delta z}\frac{\partial\int_{-\gamma}^{½\Delta z}(uv)dz}{\partial y}\right)= \qquad (11.8)$$

$$\frac{1}{4\Delta y}\left(\frac{\gamma^*_{j,k,l}}{\bar{\gamma}^*_{j,k,l}}+\frac{\gamma^*_{j+1,k,l}}{\bar{\gamma}^*_{j,k,l}}+\frac{\gamma^*_{j,k+1,l}}{\bar{\gamma}^*_{j,k,l}}+\frac{\gamma^*_{j+1,k+1,l}}{\bar{\gamma}^*_{j,k,l}}\right)\bar{u}\bar{v}_{j,k,l}$$

$$-\frac{1}{4\Delta y}\left(\frac{\gamma^*_{j,k,l}}{\bar{\gamma}^*_{j,k,l}}+\frac{\gamma^*_{j+1,k,l}}{\bar{\gamma}^*_{j,k,l}}+\frac{\gamma^*_{j,k-1,l}}{\bar{\gamma}^*_{j,k,l}}+\frac{\gamma^*_{j+1,k-1,l}}{\bar{\gamma}^*_{j,k,l}}\right)\bar{u}\bar{v}_{j,k-1,l}$$

$$FDS\left(\frac{1}{\gamma+½\Delta z}\frac{\partial\int_{-\gamma}^{½\Delta z}(uw)dz}{\partial z}\right)=\frac{\frac{\Delta z}{\bar{\gamma}^*_{j,k,l}}uw\big|_{½\Delta z}-\frac{\Delta z}{\bar{\gamma}^*_{j,k,l}}(uw)\big|_{-\gamma}(\equiv 0)}{\Delta z}$$

$$FDS\left(\frac{1}{\gamma+½\Delta z}\frac{\partial}{\partial x}\left(\nu_T\left(\frac{\int_{-\gamma}^{½\Delta z}udz}{\partial x}+\frac{\int_{-\gamma}^{½\Delta z}udz}{\partial x}\right)\right)\right)= \tag{11.9}$$

$$\frac{\frac{\gamma^*_{j+1,k,l}}{\bar{\gamma}^*_{j,k,l}}\left(u_{j+1,k,l}-u_{j,k,l}\right)\nu_{Tj+1,k,l}-\frac{\gamma^*_{j,k,l}}{\bar{\gamma}^*_{j,k,l}}\left(u_{j,k,l}-u_{j-1,k,l}\right)\nu_{Tj+1,k,l}}{\left(\Delta x\right)^2}$$

$$FDS\left(\frac{1}{\gamma+½\Delta z}\frac{\partial}{\partial y}\left(\nu_T\left(\frac{\int_{-\gamma}^{½\Delta z}udz}{\partial y}+\frac{\int_{-\gamma}^{½\Delta z}vdz}{\partial x}\right)\right)\right)=$$

$$\frac{\left(\frac{1}{2}\left(\frac{\gamma^*_{j,k+1,l}}{\bar{\gamma}^*_{j,k,l}}+\frac{\gamma^*_{j+1,k+1,l}}{\bar{\gamma}^*_{j,k,l}}\right)u_{j,k+1,l}-\frac{1}{2}\left(\frac{\gamma^*_{j,k,l}}{\bar{\gamma}^*_{j,k,l}}+\frac{\gamma^*_{j+1,k,l}}{\bar{\gamma}^*_{j,k,l}}\right)u_{j,k,l}\right)\bar{\nu}_{Tj,k,l}}{\left(\Delta y\right)^2}$$

$$\frac{\left(\frac{1}{2}\left(\frac{\gamma^*_{j,k,l}}{\bar{\gamma}^*_{j,k,l}}+\frac{\gamma^*_{j+1,k,l}}{\bar{\gamma}^*_{j,k,l}}\right)u_{j,k,l}-\frac{1}{2}\left(\frac{\gamma^*_{j,k-1,l}}{\bar{\gamma}^*_{j,k,l}}+\frac{\gamma^*_{j+1,k-1,l}}{\bar{\gamma}^*_{j,k,l}}\right)u_{j,k-1,l}\right)\bar{\nu}_{Tj,k-1,l}}{\left(\Delta y\right)^2} \tag{11.10}$$

$$\frac{\left(\frac{1}{2}\left(\frac{\gamma^*_{j+1,k,l}}{\bar{\gamma}^*_{j,k,l}}+\frac{\gamma^*_{j+1,k+1,l}}{\bar{\gamma}^*_{j,k,l}}\right)\nu_{j+1,k,l}-\frac{1}{2}\left(\frac{\gamma^*_{j,k,l}}{\bar{\gamma}^*_{j,k,l}}+\frac{\gamma^*_{j,k+1,l}}{\bar{\gamma}^*_{j,k,l}}\right)\nu_{j,k,l}\right)\bar{\nu}_{Tj,k,l}}{\Delta x\Delta y}$$

$$\frac{\left(\frac{1}{2}\left(\frac{\gamma^*_{j+1,k,l}}{\bar{\gamma}^*_{j,k,l}}+\frac{\gamma^*_{j+1,k-1,l}}{\bar{\gamma}^*_{j,k,l}}\right)\nu_{j+1,k-1,l}-\frac{1}{2}\left(\frac{\gamma^*_{j,k,l}}{\bar{\gamma}^*_{j,k,l}}+\frac{\gamma^*_{j,k-1,l}}{\bar{\gamma}^*_{j,k,l}}\right)\nu_{j,k-1,l}\right)\bar{\nu}_{Tj,k-1,l}}{\Delta x\Delta y}$$

$$FDS\left(\frac{1}{\gamma+½\Delta z}\frac{\partial}{\partial z}\left(\nu_T\left(\frac{\int_{-\gamma}^{½\Delta z} udz}{\partial z}+\frac{\int_{-\gamma}^{½\Delta z} wdz}{\partial z}\right)\right)\right)=$$

$$\frac{\frac{\Delta z}{\bar{\gamma}^*_{j,k,l}}\left(u_{j,k,l+1}-u_{j,k,l}\right)\bar{\nu}_{Tj,k,l}-\frac{\Delta}{\bar{\gamma}^*_{j,k,l}}\left[\left(u_{j,k,l}-u_{j-1,k,l-1}\right)\bar{\nu}_{Tj+1,k,l}\right](\equiv \tau b)}{(\Delta z)^2} \tag{11.11}$$

$$+\frac{\frac{\Delta z}{\bar{\gamma}^*_{j,k,l}}\left(w_{j+1,k,l}-w_{j,k,l}\right)\bar{\nu}_{Tj,k,l}-\frac{\Delta z}{\bar{\gamma}^*_{j,k,l}}\left[\left(w_{j+1,k,l-1}-w_{j,k,l-1}\right)\bar{\nu}_{Tj,k,l-1}\right](\equiv 0)}{\Delta x\Delta z}$$

The y-momentum equation yields,

$$FDS\left(\frac{1}{\gamma+½\Delta z}\frac{\partial\int_{-\gamma}^{½\Delta z}(uv)dz}{\partial x}\right)=$$

$$\frac{1}{4\Delta x}\left(\frac{\gamma^*_{j,k,l}}{\overline{\gamma^*}_{j,k,l}}+\frac{\gamma^*_{j,k+1,l}}{\overline{\gamma^*}_{j,k,l}}+\frac{\gamma^*_{j+1,k,l}}{\overline{\gamma^*}_{j,k,l}}+\frac{\gamma^*_{j+1,k+1,l}}{\overline{\gamma^*}_{j,k,l}}\right)\overline{uv}_{j,k,l}$$

$$-\frac{1}{4\Delta x}\left(\frac{\gamma^*_{j,k,l}}{\overline{\gamma^*}_{j,k,l}}+\frac{\gamma^*_{j,k+1,l}}{\overline{\gamma^*}_{j,k,l}}+\frac{\gamma^*_{j-1,k,l}}{\overline{\gamma^*}_{j,k,l}}+\frac{\gamma^*_{j-1,k+1,l}}{\overline{\gamma^*}_{j,k,l}}\right)\overline{uv}_{j-1,k,l}$$

$$FDS\left(\frac{1}{\gamma+½\Delta z}\frac{\partial\int_{-\gamma}^{½\Delta z}(vv)dz}{\partial y}\right)= \qquad (11.12)$$

$$\frac{\frac{\gamma^*_{j,k+1,l}}{\overline{\gamma^*}_{j,k,l}}\left(v_{j,k+1,l}+v_{j,k,l}\right)^2-\frac{\gamma^*_{j,k,l}}{\overline{\gamma^*}_{j,k,l}}\left(v_{j,k,l}+v_{j,k-1,l}\right)^2}{4\Delta y}$$

$$FDS\left(\frac{1}{\gamma+½\Delta z}\frac{\partial\int_{-\gamma}^{½\Delta z}(vw)dz}{\partial z}\right)=$$

$$\frac{\frac{\Delta z}{\overline{\gamma^*}_{j,k,l}}vw\Big|_{½\Delta z}-\frac{\Delta z}{\overline{\gamma^*}_{j,k,l}}(uw)\Big|_{-\gamma}\ (\equiv 0)}{\Delta z}$$

$$FDS\left(\frac{1}{\gamma+½\Delta z}\frac{\partial}{\partial x}\left(\nu_T\left(\frac{\int_{-\gamma}^{½\Delta z} v\,dz}{\partial x}+\frac{\int_{-\gamma}^{½\Delta z} u\,dz}{\partial y}\right)\right)\right)=$$

$$\frac{\left(\frac{1}{2}\left(\frac{\gamma^*_{j+1,k,l}}{\bar{\gamma}^*_{j,k,l}}+\frac{\gamma^*_{j+1,k+1,l}}{\bar{\gamma}^*_{j,k,l}}\right)v_{j+1,k,l}-\frac{1}{2}\left(\frac{\gamma^*_{j,k,l}}{\bar{\gamma}^*_{j,k,l}}+\frac{\gamma^*_{j,k+1,l}}{\bar{\gamma}^*_{j,k,l}}\right)v_{j,k,l}\right)\bar{\nu}_{Tj,k,l}}{(\Delta x)^2}$$

$$-\frac{\left(\frac{1}{2}\left(\frac{\gamma^*_{j,k,l}}{\bar{\gamma}^*_{j,k,l}}+\frac{\gamma^*_{j,k+1,l}}{\bar{\gamma}^*_{j,k,l}}\right)v_{Tj,k,l}-\frac{1}{2}\left(\frac{\gamma^*_{j-1,k,l}}{\bar{\gamma}^*_{j,k,l}}+\frac{\gamma^*_{j-1,k+1,l}}{\bar{\gamma}^*_{j,k,l}}\right)v_{j-1,k,l}\right)\bar{\nu}_{Tj-1,k,l}}{(\Delta x)^2} \qquad (11.13)$$

$$+\frac{\left(\frac{1}{2}\left(\frac{\gamma^*_{j,k+1,l}}{\bar{\gamma}^*_{j,k,l}}+\frac{\gamma^*_{j+1,k+1,l}}{\bar{\gamma}^*_{j,k,l}}\right)u_{j,k+1,l}-\frac{1}{2}\left(\frac{\gamma^*_{j,k,l}}{\bar{\gamma}^*_{j,k,l}}+\frac{\gamma^*_{j+1,k,l}}{\bar{\gamma}^*_{j,k,l}}\right)u_{j,k,l}\right)\bar{\nu}_{Tj,k,l}}{\Delta x\Delta y}$$

$$-\frac{\left(\frac{1}{2}\left(\frac{\gamma^*_{j-1,k+1,l}}{\bar{\gamma}^*_{j,k,l}}+\frac{\gamma^*_{j,k+1,l}}{\bar{\gamma}^*_{j,k,l}}\right)u_{j-1,k+1,l}-\frac{1}{2}\left(\frac{\gamma^*_{j-1,k,l}}{\bar{\gamma}^*_{j,k,l}}+\frac{\gamma^*_{j,k,l}}{\bar{\gamma}^*_{j,k,l}}\right)u_{j-1,k,l}\right)\bar{\nu}_{j-1,k,l}}{\Delta x\Delta y}$$

$$FDS\left(\frac{1}{\gamma+½\Delta z}\frac{\partial}{\partial y}\left(\nu_T\left(\frac{\int_{-\gamma}^{½\Delta z} v\,dz}{\partial y}+\frac{\int_{-\gamma}^{½\Delta z} v\,dz}{\partial y}\right)\right)\right)= \qquad (11.14)$$

$$\frac{\frac{\gamma^*_{j,k+1,l}}{\bar{\gamma}^*_{j,k,l}}\left(v_{j,k+1,l}-v_{j,k,l}\right)v_{Tj,k+1,l}-\frac{\gamma^*_{j,k,l}}{\bar{\gamma}^*_{j,k,l}}\left(v_{j,k,l}-v_{j,k-1,l}\right)v_{Tj,k,l}}{(\Delta y)^2}$$

$$FDS\left(\frac{1}{\gamma+½\Delta z}\frac{\partial}{\partial z}\left(\nu_T\left(\frac{\int_{-\gamma}^{½\Delta z} v\,dz}{\partial z}+\frac{\int_{-\gamma}^{½\Delta z} w\,dz}{\partial y}\right)\right)\right)=$$

$$\frac{\frac{\Delta z}{\bar{\gamma}^*_{j,k,l}}\left(v_{j,k,l+1}-v_{j,k,l}\right)\bar{\nu}_{Tj,k,l}-\frac{\Delta z}{\bar{\gamma}^*_{j,k,l}}\left[\left(v_{j,k,l}-v_{j,k,l-1}\right)\bar{\nu}_{Tj,k,l-1}\right](\equiv \tau b)}{(\Delta z)^2} \qquad (11.15)$$

$$+\frac{\frac{\Delta z}{\bar{\gamma}^*_{j,k,l}}\left(w_{j,k+1,l}-w_{j,k,l}\right)\bar{\nu}_{Tj,k,l}-\frac{\Delta z}{\bar{\gamma}^*_{j,k,l}}\left[\left(w_{j,k+1,l-1}-w_{j,k,l-1}\right)\bar{\nu}_{j,k,l-1}\right](\equiv 0)}{\Delta y\Delta z}$$

The vertical sweep is in MIKE 3 started with the mass equation. Assuming that the vertical velocity below the lowermost computational point is negligible (which always is correct for γ less than ½Δz), the sweep still can be started by setting up the mass balance. Hence, the z-momentum does not need to be considered in the same manner as the x- and y-momentum equations.

Thus, basically the bottom-fitted coordinates imply that the relevant velocities in the equations are multiplied by certain factors. This is much similar to the way porosity is modelled in MIKE 3, and as such it does not constitute any numerical difficulties. Except for the horizontal cross-terms in Equations (11.8), (11.10), (11.12) and (11.13), respectively, the factors easily fit into the present coding structure of MIKE 3. The reason why some terms do not fit so well is that they require information about the seabed location along the two horizontal neighbour rows whereas this information is available already for the sweep-row. Also notice that some of the γ ratios in the second and first finite difference expressions in Equations (11.8) and (11.10), respectively, by definition add up to two times unity.

If we for sake of simplicity define a new set of variables given by

$$\begin{aligned}
\gamma'_{j,k,l} &\equiv \frac{\gamma^*_{j,k,l}}{\Delta z}\\
\overline{\gamma'}_{xj,k,l} &\equiv \frac{1}{2\Delta z}\left(\gamma^*_{j,k,l}+\gamma^*_{j+1,k,l}\right)\\
\overline{\gamma'}_{yj,k,l} &\equiv \frac{1}{2\Delta z}\left(\gamma^*_{j,k,l}+\gamma^*_{j,k+1,l}\right)
\end{aligned} \qquad (11.16)$$

the set of finite difference expressions may be rewritten in a slightly different form,

$$\frac{1}{\rho c_s^2}\frac{\Delta P_{j,k,l}}{\Delta t} + \frac{u_{j,k,l}\dfrac{\bar{\gamma}'_{xj,k,l}}{\gamma'_{j,k,l}} - u_{j-1,k,l}\dfrac{\bar{\gamma}'_{j-1,k.l}}{\gamma'_{j,k,l}}}{\Delta x}$$

$$+ \frac{v_{j,k,l}\dfrac{\bar{\gamma}'_{yj,k,l}}{\gamma'_{j,k,l}} - v_{j,k-1,l}\dfrac{\bar{\gamma}'_{yj,k-1.l}}{\gamma'_{j,k,l}}}{\Delta y} \qquad (11.17)$$

$$+ \frac{w_{j,k,l}\dfrac{1}{\gamma'_{j,k,l}} - w\gamma\,(\equiv 0)\dfrac{1}{\gamma'_{j,k,l}}}{\Delta z} = SS$$

The x-momentum terms can accordingly be expressed as,

$$FDS\left(\frac{1}{\gamma+½\Delta z}\frac{\partial\int_{-\gamma}^{½\Delta z}(uu)dz}{\partial x}\right)=$$

$$\frac{\frac{\gamma'_{j+1,k,l}}{\bar{\gamma}'_{xj,k,l}}\left(u_{j+1,k,l}+u_{j,k,l}\right)^2-\frac{\gamma'_{j,k,l}}{\bar{\gamma}'_{xj,k,l}}\left(u_{j,k,l}+u_{j-1,k,l}\right)^2}{4\Delta x}$$

$$FDS\left(\frac{1}{\gamma+½\Delta z}\frac{\partial\int_{-\gamma}^{½\Delta z}(uv)dz}{\partial y}\right)= \tag{11.18}$$

$$\frac{\frac{1}{2}\left(1+\frac{\gamma'_{xj,k+1,l}}{\bar{\gamma}'_{xj,k,l}}\right)\overline{uv}_{j,k,l}-\frac{1}{2}\left(1+\frac{\gamma'_{xj,k-1,l}}{\bar{\gamma}'_{xj,k,l}}\right)\overline{uv}_{j,k-1,l}}{\Delta y}$$

$$FDS\left(\frac{1}{\gamma+½\Delta z}\frac{\partial\int_{-\gamma}^{½\Delta z}(uw)dz}{\partial z}\right)=$$

$$\frac{\frac{1}{\bar{\gamma}'_{xj,k,l}}uw\big|_{½\Delta z}-\frac{1}{\bar{\gamma}'_{xj,k,l}}(uw)\big|_{-\gamma}\ (\equiv 0)}{\Delta z}$$

$$FDS\left(\frac{1}{\gamma+½\Delta z}\frac{\partial}{\partial x}\left(\nu_T\left(\frac{\int_{-\gamma}^{½\Delta z}udz}{\partial x}+\frac{\int_{-\gamma}^{½\Delta z}udz}{\partial x}\right)\right)\right)= \tag{11.19}$$

$$\frac{\frac{\gamma'_{j+1,k,l}}{\bar{\gamma}'_{xj,k,l}}\left(u_{j+1,k,l}-u_{j,k,l}\right)\nu_{Tj+1,k,l}-\frac{\gamma'_{j,k,l}}{\bar{\gamma}'_{xj,k,l}}\left(u_{j,k,l}-u_{j-1,k,l}\right)\nu_{Tj,k,l}}{(\Delta x)^2}$$

$$FDS\left(\frac{1}{\gamma+½\Delta z}\frac{\partial}{\partial y}\left(\nu_T\left(\frac{\int_{-\gamma}^{½\Delta z}u\,dz}{\partial y}+\frac{\int_{-\gamma}^{½\Delta z}v\,dz}{\partial x}\right)\right)\right)=$$

$$\frac{\left(\frac{\bar{y}'_{xj,k+1,l}}{\bar{\gamma}'_{xj,k,l}}u_{j,k+1,l}-u_{j,k,l}\right)\bar{\nu}_{Tj,k,l}}{(\Delta y)^2}$$

$$-\frac{\left(u_{j,k,l}\frac{\bar{y}'_{xj,k-1,l}}{\bar{\gamma}'_{xj,k,l}}u_{j,k-1,l}-u_{j,k,l}\right)\bar{\nu}_{Tj,k-1,l}}{(\Delta y)^2} \qquad (11.20)$$

$$+\frac{\left(\frac{\bar{y}'_{yj+1,k,l}}{\bar{\gamma}'_{xj,k,l}}\nu_{j+1,k,l}-\frac{\bar{y}'_{yj,k,l}}{\bar{\gamma}'_{xj,k,l}}\nu_{j,k,l}\right)\bar{\nu}_{Tj,k,l}}{\Delta x\Delta y}$$

$$-\frac{\left(\frac{\bar{y}'_{yj+1,k-1,l}}{\bar{\gamma}'_{xj,k,l}}\nu_{j+1,k-1,l}-\frac{\bar{y}'_{yj,k-1,l}}{\bar{\gamma}'_{xj,k,l}}\nu_{j,k-1,l}\right)\bar{\nu}_{Tj,k-1,l}}{\Delta x\Delta y}$$

$$FDS\left(\frac{1}{\gamma+½\Delta z}\frac{\partial}{\partial z}\left(\nu_T\left(\frac{\int_{-\gamma}^{½\Delta z}u\,dz}{\partial z}+\frac{\int_{-\gamma}^{½\Delta z}w\,dz}{\partial x}\right)\right)\right)=$$

$$\frac{\frac{1}{\bar{\gamma}'_{xj,k,l}}\left(u_{j,k,l+1}-u_{j,k,l}\right)\bar{\nu}_{Tj,k,l}-\frac{1}{\bar{\gamma}'_{xj,k,l}}\left[\left(u_{j,k,l}-u_{j,k,l-1}\right)\bar{\nu}_{Tj,k,l-1}\right](\equiv \tau b)}{(\Delta x)^2} \qquad (11.21)$$

$$+\frac{\frac{1}{\bar{\gamma}'_{xj,k,l}}\left(w_{j+1,k,l}-w_{j,k,l}\right)\bar{\nu}_{Tj,k,l}-\frac{1}{\bar{\gamma}'_{xj,k,l}}\left[\left(w_{j+1,k,l-1}-w_{j,k,l-1}\right)\bar{\nu}_{Tj,k,l-1}\right](\equiv 0)}{\Delta x\Delta z}$$

The y-momentum terms may similarly be rearranged to yield,

$$FDS\left(\frac{1}{\gamma+½\Delta z}\frac{\partial\int_{-\gamma}^{½\Delta z}(uv)dz}{\partial x}\right)=$$

$$\frac{\frac{1}{2}\left(1+\frac{\gamma'_{yj+1,k,l}}{\overline{\gamma}'_{yj,k,l}}\right)\overline{uv}_{j,k,l}-\frac{1}{2}\left(1+\frac{\gamma'_{yj-1,k,l}}{\overline{\gamma}'_{yj,k,l}}\right)\overline{uv}_{j-1,k,l}}{\Delta x}$$

$$FDS\left(\frac{1}{\gamma+½\Delta z}\frac{\partial\int_{-\gamma}^{½\Delta z}(vv)dz}{\partial y}\right)=$$

$$\frac{\frac{\gamma'_{j,k+1,l}}{\overline{\gamma}'_{yj,k,l}}\left(v_{j,k+1,l}+v_{j,k,l}\right)^2-\frac{\gamma'_{j,k,l}}{\overline{\gamma}'_{yj,k,l}}\left(v_{j,k,l}+v_{j,k-1,l}\right)^2}{4\Delta y} \qquad (11.22)$$

$$FDS\left(\frac{1}{\gamma+½\Delta z}\frac{\partial\int_{-\gamma}^{½\Delta z}(vw)dz}{\partial z}\right)=$$

$$\frac{\frac{1}{\overline{\gamma}'_{yj,k,l}}vw\Big|_{½\Delta z}-\frac{1}{\overline{\gamma}'_{yj,k,l}}(uw)\Big|_{-\gamma}\ (\equiv 0)}{\Delta z}$$

$$FDS\left(\frac{1}{\gamma+½\Delta z}\frac{\partial}{\partial x}\left(\nu_T\left(\frac{\int_{-\gamma}^{½\Delta z} v\,dz}{\partial x}+\frac{\int_{-\gamma}^{½\Delta z} u\,dz}{\partial y}\right)\right)\right)=$$

$$\frac{\left(\frac{\bar{y}'_{yj+1,k,l}}{\bar{\gamma}'_{yj,k,l}}\nu_{j+1,k,l}-\nu_{j,k,l}\right)\bar{\nu}_{Tj,k,l}}{(\Delta x)^2}$$

$$-\frac{\left(\nu_{j,k,l}-\frac{\bar{y}'_{yj-1,k,l}}{\bar{\gamma}'_{yj,k,l}}\nu_{j-1,k,l}\right)\bar{\nu}_{Tj-1,k,l}}{(\Delta x)^2} \qquad (11.23)$$

$$+\frac{\left(\frac{\bar{y}'_{xj,k+1,l}}{\bar{\gamma}'_{yj,k,l}}u_{j,k+1,l}-\frac{\bar{y}'_{xj,k,l}}{\bar{\gamma}'_{yj,k,l}}u_{j,k,l}\right)\bar{\nu}_{Tj,k,l}}{\Delta x\Delta y}$$

$$-\frac{\left(\frac{\bar{y}'_{xj-1,k+1,l}}{\bar{\gamma}'_{yj,k,l}}u_{j-1,k+1,l}-\frac{\bar{y}'_{xj-1,k,l}}{\bar{\gamma}'_{yj,k,l}}u_{j-1,k,l}\right)\bar{\nu}_{Tj-1,k,l}}{\Delta x\Delta y}$$

$$FDS\left(\frac{1}{\gamma+½\Delta z}\frac{\partial}{\partial y}\left(\nu_T\left(\frac{\int_{-\gamma}^{½\Delta z} v\,dz}{\partial y}+\frac{\int_{-\gamma}^{½\Delta z} v\,dz}{\partial y}\right)\right)\right)= \qquad (11.24)$$

$$\frac{\frac{\gamma'_{j,k+1,l}}{\bar{\gamma}'_{yj,k,l}}\left(\nu_{j,k+1,l}-\nu_{j,k,l}\right)\nu_{Tj,k+1,l}-\frac{\gamma'_{j,k,l}}{\bar{\gamma}'_{yj,k,l}}\left(\nu_{j,k,l}-\nu_{j,k-1,l}\right)\nu_{Tj,k,l}}{(\Delta y)^2}$$

$$FDS\left(\frac{1}{\gamma+½\Delta z}\frac{\partial}{\partial z}\left(\nu_T\left(\frac{\int_{-\gamma}^{½\Delta z}\nu dz}{\partial z}+\frac{\int_{-\gamma}^{½\Delta z}wdz}{\partial y}\right)\right)\right)=$$

$$\frac{\frac{1}{\bar{\gamma}'_{yj,k,l}}\left(\nu_{j,k,l+1}-\nu_{j,k,l}\right)\bar{\nu}_{Tj,k,l}-\frac{1}{\bar{\gamma}'_{yj,k,l}}\left[\left(\nu_{j,k,l}-\nu_{j,k,l-1}\right)\bar{\nu}_{Tj,k,l-1}\right](\equiv \tau b)}{(\Delta z)^2} \tag{11.25}$$

$$+\frac{\frac{1}{\bar{\gamma}'_{yj,k,l}}\left(w_{j,k+1,l}-w_{j,k,l}\right)\bar{\nu}_{Tj,k,l}-\frac{1}{\bar{\gamma}'_{yj,k,l}}\left[\left(w_{j,k+1,l-1}-w_{j,k,l-1}\right)\bar{\nu}_{Tj,k,l-1}\right](\equiv 0)}{\Delta y\Delta z}$$

11.3.3 Conservation of A Scalar Quantity

The finite difference formulation of the transport equation (11.5) reads,

$$\frac{\Delta C}{\Delta t}=-\frac{\frac{\bar{\gamma}'_{x\,j,k,l}}{\gamma'_{j,k,l}}T_{x\,j,k,l}-\frac{\bar{\gamma}'_{x\,j-1,k,l}}{\gamma'_{j,k,l}}T_{x\,j-1,k,l}}{\Delta x}$$

$$-\frac{\frac{\bar{\gamma}'_{y\,j,k,l}}{\gamma'_{j,k,l}}T_{y\,j,k,l}-\frac{\bar{\gamma}'_{y\,j-1,k,l}}{\gamma'_{j,k,l}}T_{y\,j,k-1,l}}{\Delta y} \tag{11.26}$$

$$-\frac{\frac{1}{\gamma'_{j,k,l}}T_{z\,j,k,l}-\frac{1}{\gamma'_{j,k,l}}T_{z\,j,k,l-1}}{\Delta z}+SS$$

where T_x, T_y and T_z are the transports in the three directions, respectively.

12 Nesting Facility, Scientific Background

The hydrodynamic module of MIKE 3 is a general numerical modelling system for the simulation of water level variations and flows. It simulates unsteady three-dimensional flows in fluids when presented with the bathymetry and relevant conditions (e.g. bed resistance, wind field, baroclinic forcing, hydrographic boundary conditions). The nested version of MIKE 3 HD (MIKE 3 NHD) has a built-in refinement-of-scale facility, which gives a possibility of making an increase in resolution in areas of special interest.

Please note: The present “Scientific Background” section only covers description of the nesting facility in the “classic” non-hydrostatic version of the MIKE 3 NHD. For a description of the nesting facility in the hydrostatic version of MIKE 3, please see the documentation of the hydrostatic version.

As with the standard MIKE 3 HD, the mathematical foundation in MIKE 3 NHD is the mass conservation equation, the Reynolds-averaged Navier-Stokes equations, including the effects of turbulence and variable density, together with the conservation equations for salinity and temperature, see *Chapter 2: Main Equations.*

The equations are spatially discretised on a rectangular, staggered grid, the so-called Arakawa C-grid, as depicted in Figure 3.1. Scalar quantities, such as pressure, salinity and temperature, are defined in the grid nodes whereas velocity components are defined halfway between adjacent grid nodes in the respective directions.

Time centring of the hydrodynamic equations is achieved by defining pressure P at one-third time step intervals (i.e. n+1/6, n+3/6, n+5/6, etc.), the velocity component in the x-direction u at integer time levels (n, n+1, n+2, etc.), the velocity component in the y-direction v at time levels n+1/3, n+4/3, n+7/3, etc., and the velocity component in the z-direction w at time levels n+2/3, n+5/3, n+8/3, etc.

Using these discretisations, the governing partial differential equations are formulated as a system of implicit expressions for the unknown values at the grid points, each expression involving known but also unknown values at other grid points and time levels.

The applied algorithm is a non-iterative Alternating Direction Implicit (ADI) algorithm, using a "fractional step" technique (basically the time staggering described above) and "side-feeding" (semi-linearisation of non-linear terms). The resulting tri-diagonal system of equations is solved by the well-known double sweep algorithm. The reader is referred to earlier sections for an in-depth description of the numerical formulation used in the hydrodynamic modules.

The method applied to ensure the dynamical nesting in MIKE 3 NHD, i.e. the two-way dynamically exchange of mass and momentum between the modelling grids of different resolution, is a relatively simple extension of the solution method used in the standard hydrodynamic module and it may basically be described as:

Along common grid lines, see Figure 12.1, the mass and momentum equations (in the staggered grids) are dynamically connected across the borders by first setting up all coefficients for the double sweep algorithm in both coarse and fine grids. Hereafter the tri-diagonal system of equations is established.

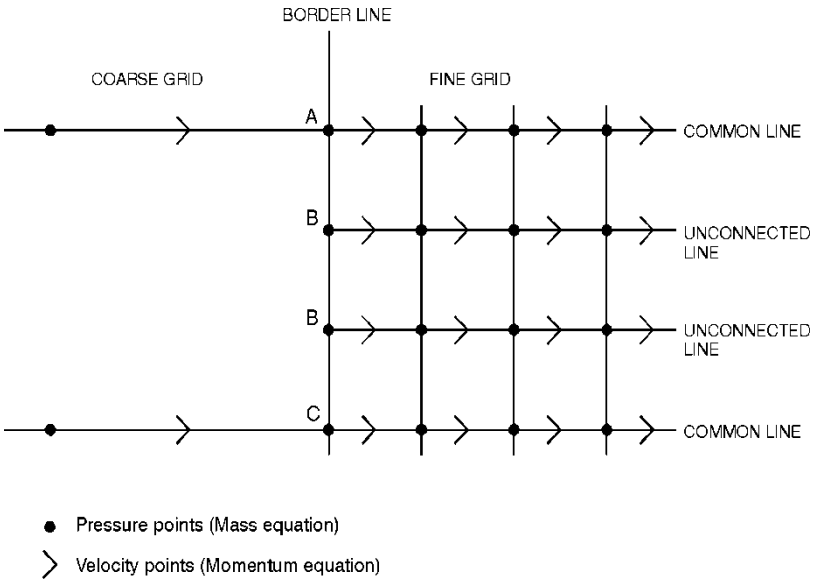

Figure 12.1 Coupling across a border line between coarse and fine staggered grid during an x-sweep.

At the end points (points B in Figure 12.1) of the two unconnected grid lines in the fine grid, between the connected grid lines, a level (i.e. pressure) boundary condition is applied. The pressure boundary values are found by assuming that $\partial P/\partial t$ in the common mass point (point A in a down-sweep and point C in an up-sweep due to the applied ADI technique) on the border of the connected grid line is identical to $\partial P/\partial t$ at the end point (mass point B) of the unconnected grid line.

At the borders, explicit parameters and values of the prognostic variables at old time steps are found by interpolation between the fine grid and the coarse grid.
In MIKE 3 NHD, the equations for all the different spatial scales in the actual model are solved at the same time. As for the standard MIKE 3 HD, the computations are divided into two parts:

- the coefficient sweeps (traditionally referred to as EF sweeps), and
- the SP- or SQ-sweeps (a traditional notation inherited from MIKE 21 NHD: *S* for surface elevation, *P* and *Q* for the two fluxes)

according to the double sweep algorithm.

The horizontal sweep structure for the hydrodynamic module in the nested version of MIKE 3 is described in the following. Remember that the nesting is in the horizontal direction only. For the vertical direction, the sweeps are conducted as for the standard MIKE 3 HD.

For odd time steps, the computations start in the upper-right corner with an x-sweep moving down in the model, followed by a y-sweep moving left in the model. These sweeps are referred to as down-sweeps. For even time steps so-called up-sweeps are performed, i.e. the computations start in the lower-right corner with an x-sweep moving up in the model, followed by a y-sweep moving right in the model. The superior computation structure is shown in Figure 12.2.

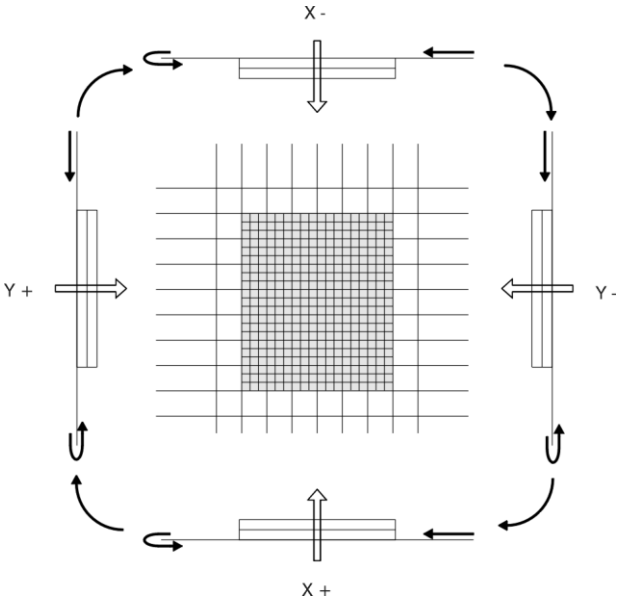

Figure 12.2 Superior structure of the computations for the nested MIKE 3 HD. X and Y indicate the sweep-direction, - indicates down-sweeps, + indicates up-sweeps.

The detailed computation structure for a down-sweep (odd time step) in the x-direction is shown in Figure 12.3. The equations at the different scales are solved at the same time. Thus, information can travel in two directions: Effects from the coarse grid influence the solution in the fine grids but also the effects in the fine grids can influence the solution in the coarse grid.

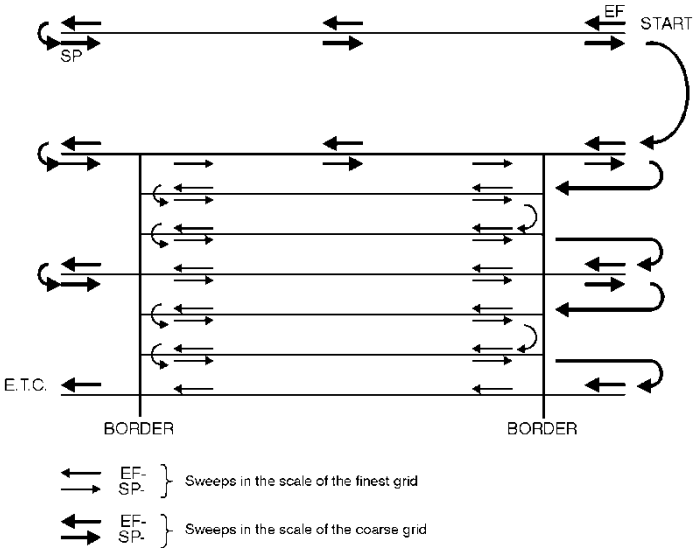

Figure 12.3 Computation structure for a down-sweep in the x-direction. The corresponding up- or y-sweeps are symmetrical.

13 References

Abbott, M.B., Computational Hydraulics - Elements of the Theory of Free Surface Flows, Pitman, London, 1979.

Chorin, A.J., A Numerical Method for Solving Incompressible Viscous Flow Problems, J. Comp. Physics, 2, 12-26, 1967.

Ferziger, J.H., Simulation of Incompressible Turbulent Flows, J. Comp. Physics, 69, 1-48, 1987.

Leendertse, J.J., Aspects of a Computational Model for Long Water Wave Propagation, Rand. Corp., RH-5299-RR, Santa Monica, California, 1967.

Leonard, B.P., A Survey of Finite Difference of Opinion on Numerical Muddling of the Incomprehensible Defective Confusion Equation, Proc. Am. Soc. Mech. Eng., Winter Annual Meeting, Publ. No. AMD-34, 1979.

Patankar, S.V., Numerical Heat Transfer and Fluid Flow, McGraw-Hill, New York, 1980.

Rasmussen, E.B., Three Dimensional Hydrodynamic Models, In Abbott, M.B. and Price, N.A. (eds), Coastal, Esturial and Harbour Engineer's Reference Book, Chapman and Hall, London, 1993.

Richtmeyer, R.D. and Morton, K.W., Difference Methods for Initial Value Problems, 2nd Ed., Interscience, New York, 1967.

Smith, S.D. and Banke, E.G., Variation of the sea drag coefficient with wind speed, Quart. J.R. Met.Soc., 101, pp. 665-673, 1975.

UNESCO, The practical salinity scale 1978 and the international equation of state of seawater 1980, Unesco technical papers in marine science, 36, 1981.

13.1 Suggestions for Further Reading

13.1.1 Hydraulics in General

Chow, Te Ven. *Open-Channel Hydraulics*, McGraw-Hill, New York, 1959.

Lamb, Horace. *Hydrodynamics*, Dover, New York, 1945.

Milne-Thomson, L.M. *Theoretical Hydrodynamics*, Macmillan, New York, 1950.

Phillips, O.M. *The Dynamics of the Upper Ocean*, Cambridge University Press, 1966.

Rouse, H. *Elementary Mechanics of Fluids*, John Wiley and Sons, New York, 1946.

Rouse, H. (editor). *Advanced Mechanics of Fluids*, Wiley, New York, 1959.

Schlichting, H. *Boundary Layer Theory*, McGraw-Hill, New York, 1960.

Streeter, V.L. *Handbook of Fluid Dynamics*, McGraw-Hill, London, 1961.

Svendsen, I.A. and Jonsson, I.G. *Hydrodynamics of Coastal Regions*, Technical University of Denmark, 1976.

U.S. Army Coastal Engineering Research Center. *Shore Protection Manual*, 1984.

13.1.2 Computational Hydraulics

Abbott, M.B. *Computational Hydraulics, Elements of the Theory of Free Surface Flows*, Pitman, London, 1979.

Abbott, M.B. and Basco, D.R. *Computational Fluid Dynamics, an Introduction for Engineers*, Longman, London, and Wiley, New York, 1989.

Abbott, M.B. and Cunge, J.A. *Engineering Applications of Computational Hydraulics*, Pitman, London, 1982.

Abbott, M.B., McCowan, A.D. and Warren, I.R. Numerical Modelling of Free-Surface Flows that are Two-Dimensional in Plan, *Transport Models for Inland and Coastal Waters*, edited by Fischer, H.B., Academic Press, New York, 1981.

Abbott, M.B. and Price, N.A. (eds.) *Coastal, Esturial and Habour Engineer's Reference Book*, Chapman and Hall, London, 1993.

Casulli, V. A Semi-Implicit Finite Difference Method for Non-Hydrostatic, Free-Surface Flows, *International Journal for Numerical Methods in Fluids,* **30**, pp 425-440, 1999.

Casulli, V. and Cattani, E. Stability, Accuracy and Efficiency of a Semi-Implicit Method for Three-Dimensional Shallow Water Fow, *Computers and Mathematics with Applications,* **27**, No. 4, pp 99-112, 1994.

Casulli, V. and Stelling, G.S. Numerical Simulation of 3D Quasi-Hydrostatic, Free-Surface Flows, *Journal of Hydraulic Engineering,* **124**, No. 7, pp 678-686, 1998.

Justesen, P., Ellegaard, A.C., Bernitt, L. and Lu, Q.-M. 2-D and 3-D Modelleing og Hong Kong Waters. In Chwang, A.T., Lee, J.H.W. and Leung, D.Y.C. (eds.): *Hydrodynamics, Theory and Applications*, *Proceedings of the second international conference on hydrodynamics, Hong Kong, 16-19 December, 1996*. Balkema, Rotterdam, 1996.

Leonard, B.P. A Stable and Accurate Convective Modelling Procedure Based on Upstream Interpolation, *Computational Methods in Applied Mechanical Engineering*, **19**, pp 59-98, 1979.

Leonard, B.P. Simple High Accuracy Resolution Program for Convective Modelling of Discontinuities, *International Journal for Numerical Methods in Fluids*, **8**, pp 1291-1318, 1988.

Marshall, J., Hill, C., Perelmann, L. and Adcroft, A. Hydrostatic, Quasi-Hydrostatic and Non-Hydrostatic Ocean Modelling, *Journal of Geophysical Research*, **Vol. 102**, No. C3, pp 5733-5752, 1997.

Pietrzak, J., Jakobson, J.B., Burchard, H., Vested, H.J. and Petersen, O. A Three Dimensional Hydrostatic Model for Coastal and Ocean Modelling using a Generalised Topography following Co-ordinate System, submitted to *Ocean Modelling*, June 2001.

13.1.3 Turbulence

Abbott, M.B. and Larsen, J. Modelling Circulations in Depth-integrated Flows, *Journal of Hydraulic Research*, **23**, pp 309-326 and 397-420, 1985.

ASCE Task Committee on Turbulence Models in Hydraulic Computations. Turbulence Modelling of Surface Water Flow and Transport, Part I-V, *Journal of Hydraulic Engineering*, **114**, No. 9, pp 970-1051, 1988.

Aupoix, B. Eddy Viscosity Subgrid Scale Models for Homogeneous Turbulence, in *Macroscopic Modelling of Turbulent Flow*, Lecture Notes in Physics, Proc. Sophie-Antipolis, France, 1984.

Burchard, H. and Baumert, H. On the performance of a mixed-layer model based on the k-ε turbulence closure, *J.Geophysical Research*, **Vol.100**, No.C5, pp 8523-8540, 1995.

Falconer, R.A. and Mardapitta-Hadjipandeli, Fernando. Bathymetric and Shear Stress Effects on an Island's Wake: A computational Study, *Coastal Engineering*, **11**, pp 57-86, 1987.

Horiuti, K. Comparison of Conservative and Rotational Forms in Large Eddy Simulation of Turbulent Channel Flow, *Journal of Computational Physics*, **71**, pp 343-370, 1987.

Laander, B.E. and Spalding, D.B. The Numerical Computation of Turbulent Flows, *Computer Methods in Applied Mechanics and Engineering*, **3**, pp 269-289, 1973.

Leonard, A. Energy Cascades in Large-Eddy Simulations of Turbulent Fluid Flows, *Advances in Geophysics*, **18**, pp 237-247, 1974.

Lilly, D.K. On the Application of the Eddy Viscosity Concept in the Inertial Subrange of Turbulence, *NCAR Manuscript No. 123*, National Center for Atmospheric Research, Boulder, Colorado, 1966.

Madsen, P.A., Rugbjerg, M. and Warren, I.R. Subgrid Modelling in Depth Integrated Flows, *Coastal Engineering Conference*, **1**, pp 505-511, Malaga, Spain, 1988.

Rodi, W. Turbulence Models and Their Application in Hydraulics - A State of the Art Review, *Special IAHR Publication*, 1980.

Rodi, W. Examples of Calculation Methods for Flow and Mixing in Stratified Fluids, *Journal of Geophysical Research*, **92**, (C5), pp 5305-5328, 1987.

Smagorinsky, J. General Circulation Experiment with the Primitive Equations, *Monthly Weather Review*, **91**, No. 3, pp 99-164, 1963.

Wang, J.D. Numerical Modelling of Bay Circulation, *The Sea, Ocean Engineering Science*, **9**, Part B, Chapter 32, pp 1033-1067, 1990.

13.1.4 Tidal Analysis

Doodson, A.T. and Warburg, H.D. *Admiralty Manual of Tides*, Her Majesty's Stationary Office, London, 1941.

Dronkers, J.J. *Tidal Computations*, North-Holland Publishing Company, Amsterdam, 1964.

Godin, G. *The Analysis of Tides*, Liverpool University Press, 1972.

Pugh, D.T. *Tides, Surges and Mean Sea-Level, A Handbook for Engineers and Scientists*, Wiley, UK, 1987.

Schwiderski, E.W. *Global Ocean Tides, Part I-X*, Naval Surface Weapons Center, Virginia, USA, 1978.

13.1.5 Wind Conditions

Duun-Christensen, J.T. The Representation of the Surface Pressure Field in a Two-Dimensional Hydrodynamic Numerical Model for the North Sea, the Skagerak and the Kattegat, *Deutsche Hydrographische Zeitschrift*, **28**, pp 97-116, 1975.

NOAA, National Weather Service. *Revised Standard Project Hurricane Criteria for the Atlantic and Gulf Coasts of the United States*, Hurricane Research Memorandum HUR 7-120, 1972.

Smith, S.D. and Banke, E.G. Variation of the Sea Drag Coefficient with Wind Speed, *Quart. J. R. Met. Soc.*, **101**, pp 665-673, 1975.

U.S. Weather Bureau. *Meteorological Characteristics of the Probable Maximum Hurricane, Atlantic and Gulf Coasts of the United States*, Hurricane Research Interim Report, HUR 7-97 and HUR 7-97A, 1968.

13.1.6 Stratified Flows

Gross, E.S., J.R.Koseff, and S.G.Monismith: Three-Dimensional Salinity Simulation of South San Fransco Bay, *Journal of Hydraulic Engineering,* **125**, No. 11, pp 1199-1209, 1999.

Fernando, H.J.S. Turbulent Mixing in Stratified Fluids, *Annual Review of Fluid Mechanics*, **23**, pp 455-493, 1991.

Munk, W.H. and Anderson, E.R. Notes on the Theory of the Termocline, *Journal of Marine Research*, **Vol. 1**, 1948.

Officer, C.B. Physical Oceanography of Estuaries, *Wiley-Interscience*, 465 pp, 1976.

Rodi, W. Examples of Calculation Methods for Flow and Mixing in Stratified Fluids, *Journal of Geophysical Research*, **92**, (C5), pp 5305-5328, 1984.

Simpson, J.E. Gravity Currents in the Environment and in the Laboratory, *Halstead Press*, 1987.

Turner, J.S. Buoyancy Effects in Fluids, *Cambridge University Press*, 368 pp, 1973.

Vested, H.J., Berg, P. and Uhrenholdt, T. Dense Water Formation in the Northern Adriatic, *Journal of Marine Systems*, Elsevier, No. 18, pp 135-160, 1998.

13.1.7 Advection Schemes

Gross, E.S., L.Bonaventura, and G.Rosatti: Consistency with Continuity in Conservative Advective Schemes for Free Surface Models, to appear in .*International Journal for Numerical Methods in Fluids*.

Gross, E.S., V.Casulli, L.Bonaventura, and J.R.Koseff: A Semi-Implicit Method for Vertical Transport in Multidimensional Models, *International Journal for Numerical Methods in Fluids,* **28**, pp 157-186, 1998.

Gross, E.S., J.R.Koseff, and S.G.Monismith: Evaluation of Advective Schemes for Estuarine Salinity Simulations, *Journal of Hydraulic Engineering,* **125**, No. 1, pp 32-46, 1999.

Vested, H.J., P.Justesen, and L.Ekebjærg: Advection-Dispersion Modelling in Three Dimensions, *Appl. Math. Modelling*, **16**, pp 506-519, 1992.

Ekebjærg, L. and P.Justesen: An Explicit Scheme for Advection-diffusion Modelling in Two Dimensions, *Computer Methods in Applied Mechanics and Engineering*, **88**, No. 3, pp 287-297, 1991.

13.1.8 Oceanography

Csanady, G.T. Circulation in the Coastal Ocean, *D. Riedel, Norwell*, Mass, 1982.

Gill, A.E. Atmosphere-Ocean Dynamics, *Academic Press*, 1980.

Gill, A.E. Atmosphere-Ocean Dynamics, *McGraw-Hill*, 1983.

LeBlond, P.H. and Mysak, L.A. Waves in the Ocean, *Elsevier*, 602 pp, 1978.

Pugh, D.T. Tides, Surges and Mean Sea-Level, *John Wiley and Sons*, New York, 1987.

13.1.9 Equation of State of Sea Water

Kelley, D.E. Temperature-Salinity Criterion for Inhibition of Deep Convection, *Journal of Physical Oceanography*, **Vol. 24**, pp 2424-2433, 1994.

UNESCO. The Practical Salinity Scale 1978 and the International Equation of State of Sea Water 1980, *UNESCO Technical Papers on Marine Science*, 1981.